

Design and Assembly of MiniFuel Targets for Characterization of High Burnup UO_2 Specimens Irradiated in the High Flux Isotope Reactor



A. G. Le Coq
A. C. Telles
A.K. Kercher
C.A. Hobbs
T.L Ulrich
J. R. Chappell
J. P. Gorton
K. M. Godsey
C. M. Petrie
N. A. Capps

June 2024

M3FT-24OR020205034



DOCUMENT AVAILABILITY

Online Access: US Department of Energy (DOE) reports produced after 1991 and a growing number of pre-1991 documents are available free via <https://www.osti.gov>.

The public may also search the National Technical Information Service's [National Technical Reports Library \(NTRL\)](#) for reports not available in digital format.

DOE and DOE contractors should contact DOE's Office of Scientific and Technical Information (OSTI) for reports not currently available in digital format:

US Department of Energy
Office of Scientific and Technical Information
PO Box 62
Oak Ridge, TN 37831-0062
Telephone: (865) 576-8401
Fax: (865) 576-5728
Email: reports@osti.gov
Website: www.osti.gov

This report was prepared as an account of work sponsored by an agency of the United States Government. Neither the United States Government nor any agency thereof, nor any of their employees, makes any warranty, express or implied, or assumes any legal liability or responsibility for the accuracy, completeness, or usefulness of any information, apparatus, product, or process disclosed, or represents that its use would not infringe privately owned rights. Reference herein to any specific commercial product, process, or service by trade name, trademark, manufacturer, or otherwise, does not necessarily constitute or imply its endorsement, recommendation, or favoring by the United States Government or any agency thereof. The views and opinions of authors expressed herein do not necessarily state or reflect those of the United States Government or any agency thereof.

Advanced Fuels Campaign

**DESIGN AND ASSEMBLY OF MINIFUEL TARGETS FOR CHARACTERIZATION
OF HIGH BURNUP UO_2 SPECIMENS IRRADIATED
IN THE HIGH FLUX ISOTOPE REACTOR**

A. G. Le Coq
A. C. Telles
A.K. Kercher
C.A. Hobbs
T.L Ulrich
J. R. Chappell
J. P. Gorton
K. M. Godsey
C. M. Petrie
N. A. Capps

June 2024

Prepared by
OAK RIDGE NATIONAL LABORATORY
Oak Ridge, TN 37831
managed by
UT-BATTELLE LLC
for the
US DEPARTMENT OF ENERGY
under contract DE-AC05-00OR22725

CONTENTS

FIGURES.....	iv
TABLES	v
ABBREVIATIONS	vi
ACKNOWLEDGMENTS	vii
ABSTRACT.....	viii
1. INTRODUCTION	1
2. EXPERIMENT DESIGN AND ANALYSIS.....	1
2.1 EXPERIMENT TEST MATRIX.....	1
2.2 EXPERIMENT DESIGN.....	2
2.3 EXPERIMENT DESIGN RESULTS	4
3. PREPARATION OF MINIATURE FUEL SPECIMENS	6
3.1 FABRICATION OF UO ₂ DISK SPECIMENS	6
3.2 CHARACTERIZATION OF THE UO ₂ SPECIMENS	9
3.2.1 Pellet Density Measurements.....	9
3.2.2 Pellet Microstructure and Grain Size.....	9
3.2.3 Dimensional Inspection of the Disk Specimens	9
3.2.4 Summary of the Disk Specimen Pre-Characterization.....	9
4. EXPERIMENT ASSEMBLY.....	11
4.1 SUBCAPSULE ASSEMBLY.....	11
4.2 TARGET ASSEMBLY.....	12
4.3 MINIFUEL BASKET ASSEMBLY LOADING.....	15
5. HFIR INSERTION	15
5.1 HFIR APPROVAL PACKAGES	15
5.2 HFIR IRRADIATION	16
6. FUTURE WORK.....	17
7. CONCLUSIONS	17
8. REFERENCES	18
APPENDIX A. SEM IMAGES OF PELLETS.....	A-1
APPENDIX B. OM IMAGES OF PELLETS.....	B-1
APPENDIX C. OM IMAGES OF PELLETS.....	C-2
APPENDIX D. HFIR DISK SPECIMENS INSPECTION RESULTS.....	D-1

FIGURES

Figure 1. MiniFuel experiment design: (a) HFIR layout with location of the VXF and RB MiniFuel basket assembly, and (b) details of a MiniFuel target and subcapsule.	3
Figure 2. Example of time-dependent fuel specimen temperatures in HBU03 corresponding to RA position 32.....	4
Figure 3. Distribution of TAVA fuel temperatures and discharge burnups.....	6
Figure 4. Workflow to fabricate the MiniFuel specimens.	7
Figure 5. Metal furnace used to sinter green pellets.	8
Figure 6. Image of a sintered fuel pellet, a MiniFuel disk specimen, and a penny for scale.	8
Figure 7. Example of subcapsule parts layout (a) and disk fuel specimen (b).....	11
Figure 8. Subcapsule assembly step (a) and assembled subcapsules loaded into the fixture for electron beam welding (b).	12
Figure 9. Preassembly target layout for HBU03.....	13
Figure 10. MiniFuel targets fully assembled (a), and RB basket assembly parts layout (b) with fueled targets, dummy targets, and RB basket.....	15
Figure 11. RB MiniFuel basket being inserted in HFIR.	16

TABLES

Table 1. MiniFuel HBU irradiation test matrix.....	2
Table 2. HBU MiniFuel design summary.....	5
Table 3. Results of the fuel specimen pre-characterization	10
Table 4. List of specimens inserted in each target and their corresponding positions.	14
Table 5. Irradiation details for the HBU MiniFuel targets.....	17

ABBREVIATIONS

AFC	Advanced Fuels Campaign
EABD	experiment authorization basis document
EB	electron beam
EBS	ethylene bis-stearamide
EBSD	electron backscatter diffraction
FFRD	fuel fragmentation, relocation, and dispersion
GTAW	gas tungsten arc welding
HBU	high burnup
HBS	high-burnup structure
HFIR	High Flux Isotope Reactor
HGR	heat generation rate
LAMDA	Low-Activation Materials Development and Analysis
LANL	Los Alamos National Laboratory
LOCA	loss-of-coolant accident
MCNP	Monte Carlo N-Particle
NDE	nondestructive examination
OM	optical microscopy
ORIGEN	Oak Ridge Isotope Generator
ORNL	Oak Ridge National Laboratory
QA	quality assurance
PIE	post-irradiation examination
RA	radial–axial
RB	removable beryllium
SEM	scanning electron microscopy
TAVA	time-averaged, volume-averaged
TEM	transmission electron microscopy
TM	temperature monitor
UHP	ultra-high purity
VXF	vertical experiment facility

ACKNOWLEDGMENTS

This work has been funded by the Advanced Fuels Campaign, US Department of Energy, Office of Nuclear Energy. The co-authors would like to acknowledge David Bryant and Abby Till for their work on the experiment assembly.

ABSTRACT

Safety concerns have been established regarding the performance of high-burnup fuel during a loss of coolant accident, and the observed performance is coupled to the microstructural formations across the UO_2 fuel pellet. These microstructural features are a result of the radial temperature and burnup profile across the fuel pellet; an understanding of the conditions driving the formation of these features may prove critical for minimizing fuel fragmentation, relocation, and dispersal consequences. To study the effects of temperature on the microstructure of UO_2 fuel, a MiniFuel experiment was designed in the High Flux Isotope Reactor on small UO_2 disk specimens fabricated at Oak Ridge National Laboratory. The High Flux Isotope Reactor affords the opportunity to accelerate burnup in order to rapidly answer key questions associated to fuel performance. The density and grain size of the fabricated UO_2 disk specimens represent commercial UO_2 fuel pellets. The irradiation conditions selected for this experiment include a fuel average temperature ranging between 600 to 1,000°C in 100°C increments and a sample burnup ranging from 50 to 70 MWd/kgU. The goals of this experiment are (1) to investigate the burnup and temperature thresholds for dark zone formation UO_2 , (2) to explore fission rate effects on microstructure formations, and (3) to assess other fuel performance considerations such as fission gas release and unconstrained swelling under various irradiation conditions. Seven MiniFuel targets were successfully assembled and inserted into the reactor in the Removable Beryllium and Vertical Experiment Facility locations. This report summarizes the experiment design and test matrix, the fuel fabrication and pre-characterization, the target assembly, as well as the successful insertion of targets into the reactor.

1. INTRODUCTION

The nuclear industry is seeking to extend commercial reactor cycle lengths from 18 to 24 months with increased enrichment, thereby allowing the fuel to reach peak rod average burnups greater than the current operational limit of 62 MWd/kgU [1] [2]. The formation and performance of high-burnup structures (HBSs) and dark zones across UO_2 fuel pellets may pose safety concerns for high-burnup reactor designs under loss-of-coolant-accident (LOCA) conditions, thus impacting the licensing of the current nuclear reactor fleet for higher burnup. The primary technical challenges related to burnup extension are (1) to address the phenomenon of fuel fragmentation, relocation, and dispersal (FFRD), which could lead to a potential risk for public safety, and (2) to gain an understanding of how and why the HBS and dark zone form, which may help alleviate and potentially mitigate FFRD safety concerns. The local temperature and burnup across the fuel pellet may be the drivers for the observed microstructures, and when these factors are coupled with fission gas over-pressurization, mechanisms are formed which drive FFRD [3] [4]. Fine fuel fragmentation is most likely to occur in fuel regions with fully or partially restructured grains and high porosity, as shown by McKinney et al., [5]. Understanding the mechanisms driving this behavior could help identify opportunities to mitigate LOCA consequences and to optimize core designs for reactors with extended cycle lengths.

Oak Ridge National Laboratory (ORNL) has leveraged its MiniFuel irradiation capabilities [6][7] to develop an experiment with the goal to (1) investigate the dark zone formation temperature and burnup thresholds in high-burnup UO_2 fuel specimens, (2) explore fission rate effects on microstructure, and (3) assess other high-burnup fuel performance characteristics such as fission gas release and unconstrained swelling under various irradiation conditions. Miniature UO_2 fuel specimens were fabricated at ORNL to be inserted into MiniFuel targets for accelerated separate effects irradiation testing in ORNL's High Flux Isotope Reactor (HFIR). The fuel specimens are intended to be representative of commercial UO_2 pellets, with a grain size ranging from 8 to 12 μm and a minimum density of 95%. The MiniFuel targets were designed to reach discharge burnups between 50 and 73 MWd/kgU and average fuel temperatures of 600, 700, 800, 900, and 1,000°C. The targets were inserted into HFIR in either a vertical experiment facility (VXF) position or a removable beryllium (RB) position. In the RB position, the specimen fission rate is more than twice that of a VXF position.

This report summarizes experiment design and test matrix, fuel specimen fabrication and pre-characterization, and target assembly and insertion into HFIR.

2. EXPERIMENT DESIGN AND ANALYSIS

2.1 EXPERIMENT TEST MATRIX

The experiment test matrix comprises seven MiniFuel targets containing UO_2 disk specimens. The discharge burnup was intended to be at least 55 MWd/kgU, and the target average fuel temperatures are set to range from 600 to 1,000°C in 100°C increments. Most fuel specimens contain natural uranium and were fabricated at ORNL (see Section 3). Targets HBU06 and HBU07 also contain some Cr-doped UO_2 specimens fabricated from depleted uranium by Los Alamos National Laboratory (LANL). Five targets were designed for insertion into HFIR RB positions for 7 cycles, and two targets were designed for insertion into HFIR VXF positions for 16 cycles, which is the maximum number of cycles allowed in a VXF position based on current bounding (conservative) safety calculations. Both RB and VXF irradiation locations are being used to ultimately determine the impact of fission rate effects on HBS formation. **Table 1** summarizes the experiment test matrix.

Table 1. MiniFuel HBU irradiation test matrix

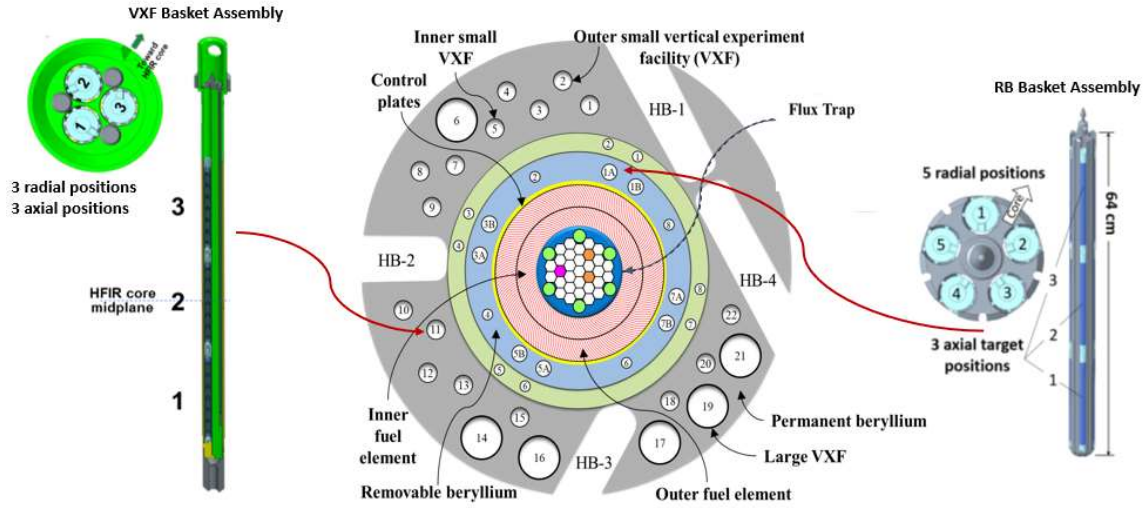
Target ID	Fuel specimens	Enrichment (wt %)	Irradiation location	Intended number of HFIR cycles	Target burnup (MWd/kg-U)	Target fuel specimen average temperatures (°C)
HBU01	UO ₂ disks	0.71%	RB	7	62–71	600, 700, 800
HBU02	UO ₂ disks	0.71%			63–72	900, 1000
HBU03	UO ₂ disks	0.71%			60–66	600, 700, 800
HBU04	UO ₂ disks	0.71%			55–60	900, 1,000
HBU05	UO ₂ disks	0.71%			60–66	600, 700, 800
HBU06	UO ₂ disks	0.71% and 0.35%*	VXF	16	50–55	600, 700, 800
HBU07	UO ₂ disks	0.71% and 0.35%*			50–55	600, 700, 800

*Targets HBU06 and HBU07 also contain depleted Cr-doped UO₂ disk specimens.

2.2 EXPERIMENT DESIGN

This experiment uses the MiniFuel irradiation platform, which has been described in the literature [6] [7] and is represented in **Figure 1**. The fuel specimens chosen for this experiment are UO₂ fuel disks measuring 3 mm in diameter and 0.3 mm thick. Each disk specimen is placed into a molybdenum (Mo) cup, or fuel dish, and inserted at the bottom of a Mo holder. A Mo tube is inserted onto the cup and acts as the heater during irradiation, generating most of the heat for the experiment via gamma heating. A silicon carbide (SiC) temperature monitor (TM) is placed inside the tube and will be used post irradiation to confirm the irradiation temperature. Grafoil disks are placed on the tops of the inner components of the subcapsules that compress during assembly to ensure that the cup remains in contact with the holder to effectively transfer heat. Finally, an end cap is welded onto the holder to create a sealed subcapsule that is backfilled with 100% helium (He) gas. Six subcapsules are stacked inside a MiniFuel target, backfilled with a mixture of He and Ar gas, and welded. The temperature of the fuel specimen is passively controlled by the gas gap between the outer wall of the subcapsule and the inner wall of the target tube. Each MiniFuel target is loaded into either the VXF or RB MiniFuel basket at its designated radial and axial (RA) position.

(a)



(b)

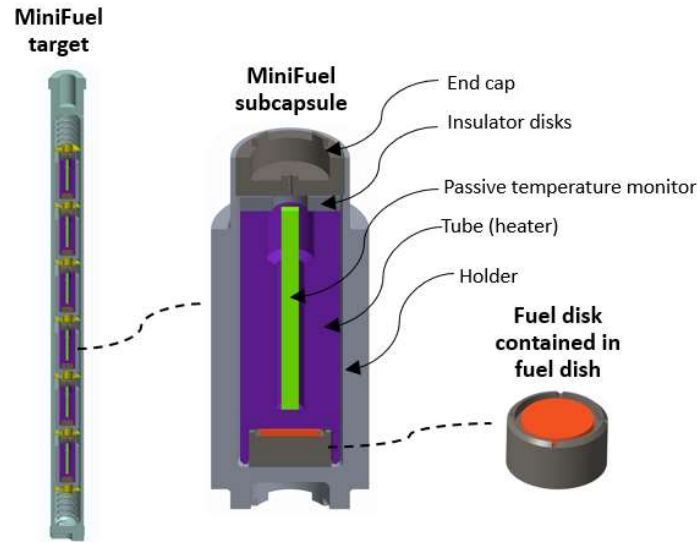


Figure 1. MiniFuel experiment design: (a) HFIR layout with location of the VXF and RB MiniFuel basket assembly, and (b) details of a MiniFuel target and subcapsule.

The neutronic and thermal design process for MiniFuel targets is described in Petrie et al., [6] and Gorton et al., [7] and is briefly reiterated here. Neutronics calculations are performed using HFIRCON [8], a wrapper code that couples the Monte Carlo N-Particle (MCNP) code [9] with the Oak Ridge Isotope Generator (ORIGEN) [10] module of the SCALE package. Coupling these tools enables heat generation rates (HGRs) to be calculated from all neutron- and gamma-induced reactions as a function of time and experiment position, and it also facilitates isotope tracking across multiple HFIR cycles. Fuel specimen burnups are also calculated using this neutronics methodology. HGRs and burnups for natural UO_2 in the RB facility were taken from a previous experiment containing bare kernel fuel geometries [11], and new calculations were performed for natural and depleted UO_2 in the VXF. Time-dependent HGRs were imported into an ANSYS [12] finite element model of a MiniFuel target to calculate temperature distributions throughout the irradiation. Three primary parameters can be varied to obtain the desired fuel temperatures: (1) the gas gap thickness between each subcapsule and target housing inner wall, (2) the

target fill gas composition (He/Ar mixture), and (3) the position of the target within the irradiation vehicle. These parameters are varied within the allowable safety bounds until the desired time-averaged, volume-averaged (TAVA) fuel temperatures are met. Because minimal axial heat transfer occurs between subcapsules, multiple fuel temperatures can be achieved within a single target. The target position is determined with consideration of the desired fuel specimen burnup and position availability.

2.3 EXPERIMENT DESIGN RESULTS

A new RB MiniFuel basket was installed for this experiment. As such, all five midplane target positions were available and selected for the RB irradiation because the midplane positions provide the highest fuel specimen fission rates and therefore the shortest irradiation times. Available midplane positions were also available and used for the two VXF targets. **Figure 2** shows an example of the time-dependent average fuel temperatures predicted by ANSYS for HBU03, which was inserted into RA position 32. **Table 2** lists the fill gas, subcapsule holder diameters, TAVA fuel temperatures, TAVA TM temperatures, and discharge burnups for all MiniFuel targets included in the irradiation. The dilatometry method used to verify the TM temperature [13][14] is biased towards the temperature incurred near the end of the irradiation. The TAVA temperature during the last irradiation cycle can differ from the full-irradiation TAVA temperature when there is a significant heat-up or cool-down period at the start of the irradiation resulting from ^{235}U depletion and ^{239}Pu breeding. This breeding/burning equilibrium is achieved quickly for natural UO_2 at the core midplane. Because the difference in fission heating before and after reaching equilibrium is minimal, the difference in last-cycle and full-irradiation TAVA TM temperatures is negligible. The TAVA fuel temperatures and discharge burnups are plotted in Figure 3 to illustrate the design envelope. The desired discharge burnups were achieved after 7 irradiation cycles in the RB positions. VXF MiniFuel experiments are currently limited to 16 cycles, so the burnups listed in Table 2 reflect the maximum achievable values for natural and depleted UO_2 .

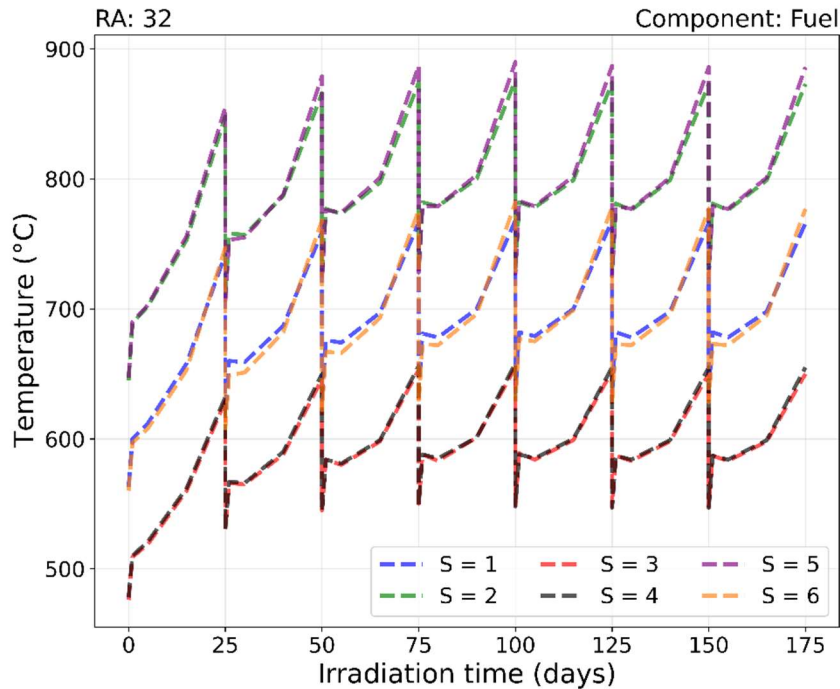


Figure 2. Example of time-dependent fuel specimen temperatures in HBU03 corresponding to RA position 32.

Table 2. HBU MiniFuel design summary

Target ID	RA position	Fill gas	S	Holder OD (mm)	TAVA fuel temperature (°C)	TAVA TM temperature (°C)	Discharge burnup (MWd/kg-U)
HBU01	12	100% He	6	9.62	603.9	511.1	68.1
			5	9.47	706.2	598.6	69.8
			4	9.31	800.2	681.8	70.6
			3	9.32	797.9	685.5	69.5
			2	9.50	701.1	606.4	67.0
			1	9.66	595.4	517.7	62.4
HBU02	22	75% He / 25% Ar	6	9.18	903.6	893.6	69.4
			5	9.46	1,007.6	790.4	71.5
			4	9.31	903.6	879.1	72.1
			3	9.51	1,006.8	784.9	70.5
			2	9.32	905.5	879.3	68.7
			1	9.47	1,012.1	792.4	63.9
HBU03	32	100% He	6	9.12	703.2	606.6	64.4
			5	8.76	804.3	700.7	65.9
			4	9.49	602.7	517.3	66.2
			3	9.52	604.1	510.1	64.9
			2	8.87	808.1	692.6	63.2
			1	9.22	701.6	608.1	59.7
HBU04	42	65% He / 35% Ar	6	9.21	1,008.8	813.1	59.7
			5	9.03	900.6	898.8	60.7
			4	9.34	1006.5	801.9	61.4
			3	9.11	904.7	893.9	60.5
			2	9.36	1,007.0	798.6	58.5
			1	9.07	910.1	898.7	55.3
HBU05	52	100% He	6	8.86	802.3	705.9	64.7
			5	9.56	604.0	516.6	66.3
			4	9.35	706.1	603.3	66.1
			3	9.35	704.3	609.1	65.8
			2	9.60	601.8	514.4	63.7
			1	9.04	806.7	693.2	59.6
HBU06	22	42% He / 58% Ar	6	9.31	598.0	557.8	54.7
			5	9.01	701.8	656.3	54.7
			4	8.61	799.4	755.3	51.7
			3	8.62	797.2	754.4	55.6
			2	8.99	701.0	663.2	55.1
			1	9.28	601.9	566.1	50.0
HBU07	32	42% He / 58% Ar	6	9.00	700.2	657.0	54.6
			5	8.51	801.8	759.1	54.4
			4	9.35	599.7	561.4	51.5
			3	8.99	699.0	657.7	55.7
			2	9.35	600.2	557.6	54.9
			1	8.48	799.4	754.3	49.9

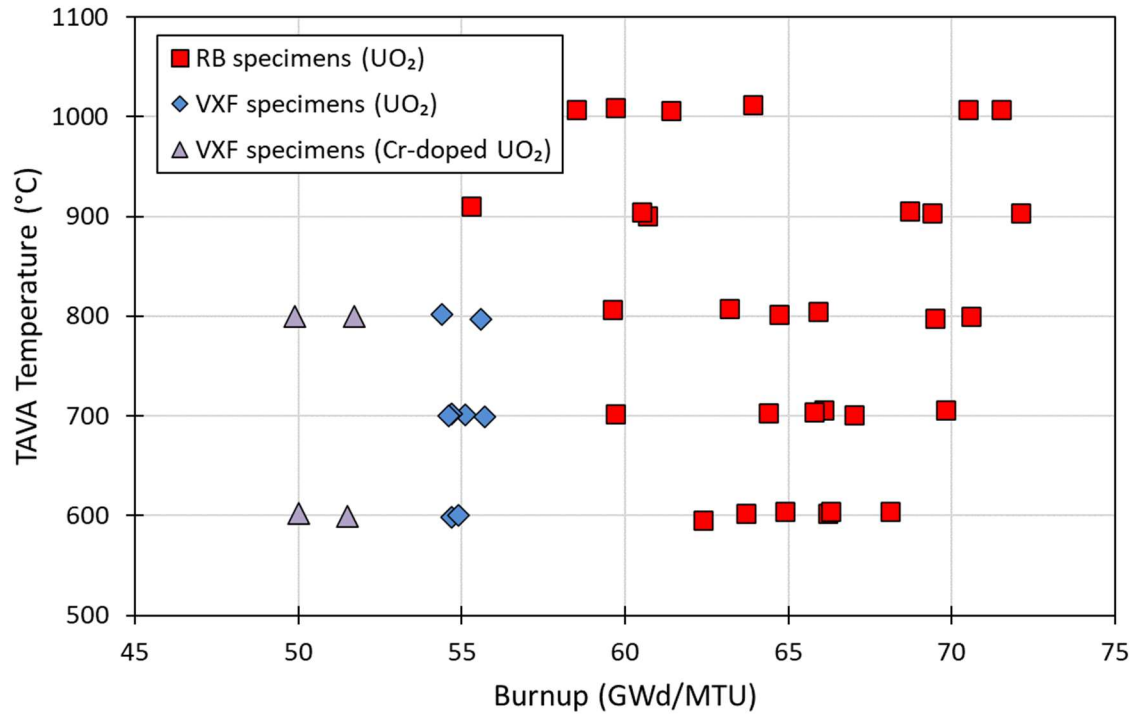
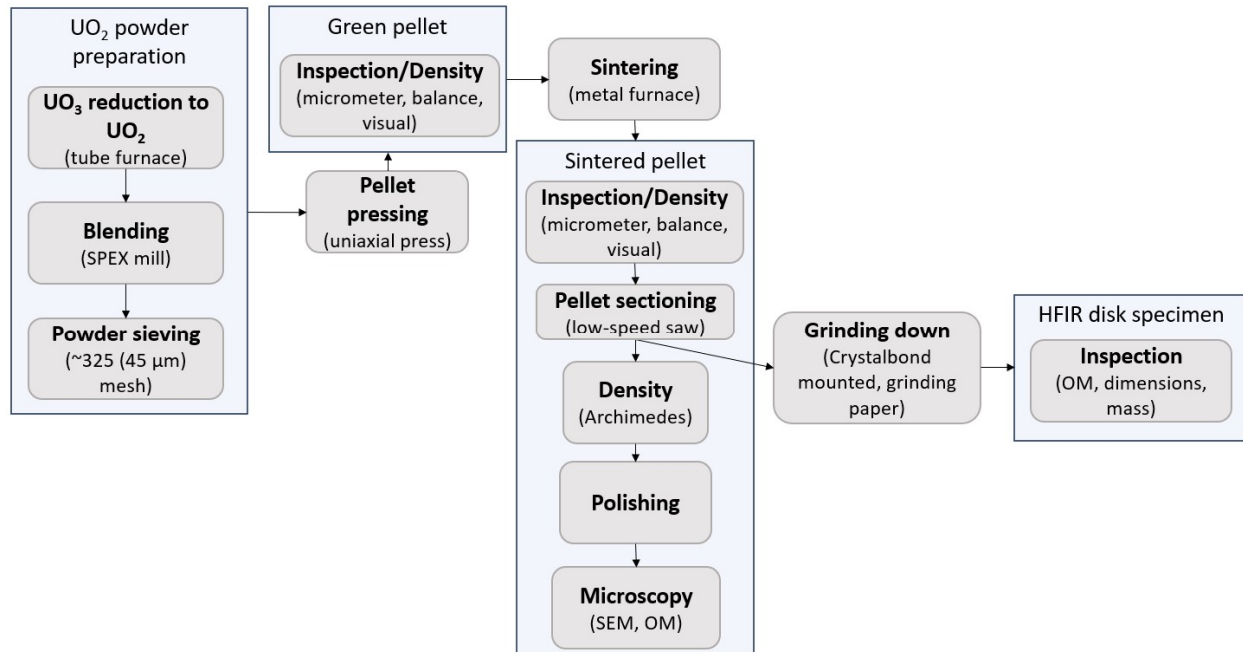


Figure 3. Distribution of TAVA fuel temperatures and discharge burnups.

3. PREPARATION OF MINIATURE FUEL SPECIMENS

3.1 FABRICATION OF UO₂ DISK SPECIMENS

The fabrication of UO₂ disk specimens was performed at ORNL and included the following major steps: (1) produce UO₂ powder by reducing UO₃ powder feedstock, (2) press and sinter pellets with the appropriate parameters (sintering time, atmosphere, and temperature) to achieve the desired grain size (8–12 μm) and density ($\geq 95\%$), and (3) polish the specimens to the desired thickness (≤ 0.4 mm) for the HFIR experiment. The fabrication process is summarized in **Figure 4** and is detailed in the fabrication procedure [15].



SEM = scanning electron microscopy; OM = optical microscopy

Figure 4. Workflow to fabricate the MiniFuel specimens.

To produce the natural UO_2 powder needed for fabrication of the MiniFuel fuel specimens, natural uranium trioxide (UO_3) powder was reduced to UO_2 in a tube furnace with a 4% H_2 -Ar balance gas environment. The weight of the powder was measured before and after the reduction to verify that the powder was fully converted. The UO_2 powder was subsequently milled in batches with an ethylene bis-stearamide (EBS) binder in a high-energy SPEX mill. The powder was milled in a zirconia crucible with yttria-stabilized zirconia milling media. After the powder was milled, it was sieved through a 325 mesh (45 micron) brass sieve to ensure uniformity. The resulting UO_2 powder was then used to fabricate pellets.

UO_2 pellets were fabricated by weighing out approximately 0.4 g of sieved powder into a stainless-steel 3.8 mm punch and die body and subsequently pressed in a manual Carver press. Stearic acid was used as a lubricant on the die body and punches to ensure the ease of pellet removal of the green body and to prevent binding of the die and punches during the pressing process. These green pellets were then sintered inside a tungsten metal furnace (see **Figure 5**) from Materials Research Furnaces LLC in an atmosphere of 4% H_2 -Ar. Pellets were sintered in three different batches on three different dates. Each batch contained ~20 pellets each. Pellets were placed in tungsten crucibles on top of a bed of UO_2 powder to avoid interaction with the crucible.

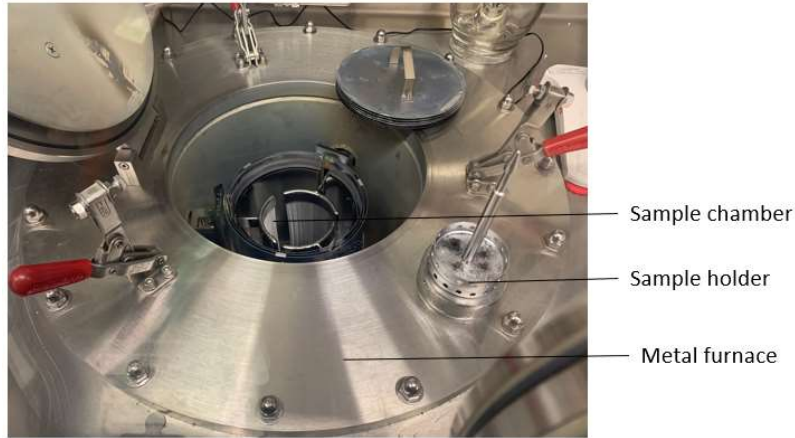


Figure 5. Metal furnace used to sinter green pellets.

The sintered pellets were sectioned using a low-speed diamond blade saw to perform some pre-characterization work (see Section 0) on one half of the pellet and to thin down the other half of the pellet to the desired specimen thickness for insertion into HFIR. The half of the pellet intended for thinning was mounted on a substrate with Crystalbond mounting adhesive. Once mounted, the half of the pellet was ground down by hand close to its final thickness using SiC grinding paper, and then it was flipped to the opposite side and again remounted with Crystalbond and polished to the final desired thickness. This work was performed on the Struers Tegra-Pol-15 with a 1 μm diamond suspension. **Figure 6** presents a sintered pellet, a MiniFuel disk specimen, and a penny for scale.

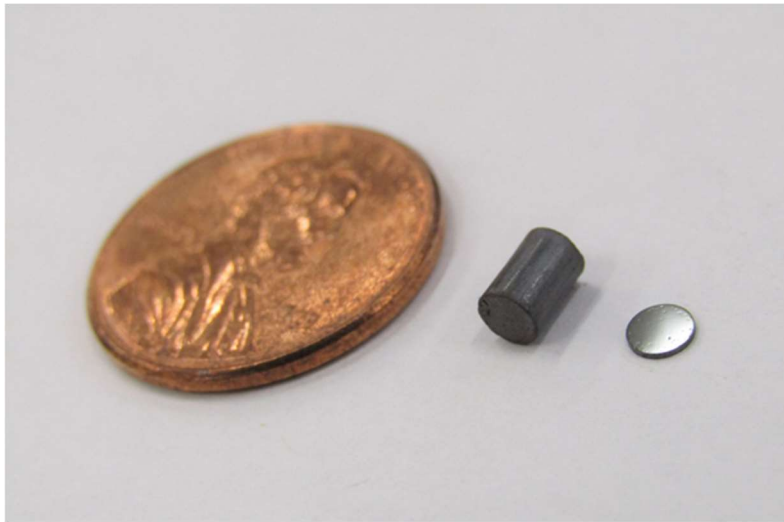


Figure 6. Image of a sintered fuel pellet, a MiniFuel disk specimen, and a penny for scale.

3.2 CHARACTERIZATION OF THE UO_2 SPECIMENS

3.2.1 Pellet Density Measurements

The geometric density of each sintered pellet was calculated from dimensional measurements with a Mitutoyo micrometer (caliper) to 0.01 mm precision, and mass measurements were taken with a Mettler Toledo analytical balance to the fourth decimal place. Sintered pellet (full or half pellets) densities were also measured using the Archimedes method by immersing the pellets in ethanol. The results of the density measurements are shown in Section 3.2.4. The theoretical density is based on the density of pure UO_2 (10.97 g/cm³). Both the dimensional and Archimedes densities correlated quite well to each other, with densities of 95% or greater. In addition, the density variation between pellets is small, within ~2%.

3.2.2 Pellet Microstructure and Grain Size

Several pellets from each sintering batch were cross sectioned, polished with a Struers TegraPol-15 polisher utilizing various Struers polishing pads and diamond suspensions. Optical microscopy (OM) and scanning electron microscopy (SEM) images were taken on some specimens of each batch to verify that there were no large defects in the pellet and to analyze the grain size, respectively. SEM and optical images are provided in Appendix A and APPENDIX B, respectively. SEM images were captured on polished surfaces of the pellet's center and on two sides. All SEM images in appendix are from the west side of each pellet. The grain size analysis was performed manually on some of the specimens utilizing the ASTM Standard E112-12 planimetric method on rectangular image regions (70.5 mm × 71 mm = 5,000 mm² rectangle). The magnifications used for this method were chosen to obtain a minimum of 50 grains within the rectangle that would be easily distinguishable. The results of this analysis are provided in Section 3.2.4, showing that the measured average grain size over the three areas of each pellet is within the desired 8–12 μm range.

3.2.3 Dimensional Inspection of the Disk Specimens

The final disk specimens that were intended for assembly in the MiniFuel experiment were inspected for diameter, thickness, and mass, using a Fowler 667955 digital caliper, a Starrett F2720-0 digital indicator, and a Mettler XP-504 analytical balance, respectively. Measurements of the thickness and the diameter were recorded at five and three locations, respectively. The average inspection results are provided in Section 3.2.4 below and the results of the various measurements are shown in APPENDIX D. The dimensions of the fuel specimens meet the design requirements of a maximum diameter of 3.4 mm and a maximum thickness of 0.4 mm.

3.2.4 Summary of the Disk Specimen Pre-Characterization

Table 3 summarizes the density, grain size, and dimensions of each MiniFuel specimen (natural UO_2) included in this irradiation. The average grain size (and corresponding standard deviation) for sintering batch #3 was calculated from grain size measurements on pellets used for HFIR specimens in addition to other pellets (back-up). Pellets UO2-HBU-MiniF-01-23060201 and -23060202 do not have Archimedes density data because they were used to analyze the grain size. These pellets are available for additional Archimedes density measurements, which can be performed in the future as needed.

Table 3. Results of the fuel specimen pre-characterization

Specimen ID	Sintering batch #	Density measured on sintered pellet			Batch average grain size (μm)	Fuel disk		
		From dimensions		From Archimedes method (% Theo. density)		Mass (g) (± 0.00012 g)	Thickness (mm) (±0.001 mm)	Diameter (mm) (±0.01 mm)
		(g/cc)	(% Theo. density)					
UO2-HBU-MiniF-01-23060201	1	10.59 ± 0.13	96.55 ± 1.22	N/A	11.86 (σ = 0.49)	0.0255	0.308	3.18
UO2-HBU-MiniF-01-23060202		10.60 ± 0.13	96.61 ± 1.22	N/A		0.0231	0.277	3.18
UO2-HBU-MiniF-01-23060203		10.68 ± 0.14	97.35 ± 1.24	95.44 ± 1.45*		0.0228	0.274	3.18
UO2-HBU-MiniF-01-23060204		10.62 ± 0.13	96.85 ± 1.23	97.97 ± 1.24*		0.0260	0.310	3.17
UO2-HBU-MiniF-01-23060205		10.57 ± 0.13	96.35 ± 1.22	96.45 ± 1.47*		0.0280	0.337	3.18
UO2-HBU-MiniF-01-23060206		10.64 ± 0.14	96.98 ± 1.23	96.77 ± 1.06*		0.0300	0.361	3.17
UO2-HBU-MiniF-01-23060207		10.74 ± 0.14	97.88 ± 1.24	96.51 ± 1.23*		0.0275	0.332	3.19
UO2-HBU-MiniF-01-23060208		10.62 ± 0.13	96.78 ± 1.22	94.57 ± 1.23*		0.0217	0.262	3.18
UO2-HBU-MiniF-01-23060609		10.61 ± 0.13	96.75 ± 1.22	94.72 ± 1.06*		0.0188	0.228	3.18
UO2-HBU-MiniF-01-23060610		10.72 ± 0.14	97.70 ± 1.24	96.10 ± 1.07*		0.0249	0.297	3.18
UO2-HBU-MiniF-01-23060611		10.57 ± 0.13	96.32 ± 1.22	96.35 ± 1.26*		0.0246	0.295	3.18
UO2-HBU-MiniF-01-23061912		10.79 ± 0.14	98.39 ± 1.24	97.74 ± 1.37*		0.0236	0.280	3.20
UO2-HBU-MiniF-01-23061913		10.66 ± 0.14	97.22 ± 1.23	95.92 ± 1.21*		0.0244	0.295	3.17
UO2-HBU-MiniF-01-23061914		10.47 ± 0.13	95.48 ± 1.20	96.65 ± 1.44*		0.0262	0.312	3.18
UO2-HBU-MiniF-01-23061915		10.59 ± 0.13	96.49 ± 1.22	95.34 ± 1.37*		0.0254	0.309	3.17
UO2-HBU-MiniF-01-23061916		10.68 ± 0.13	97.39 ± 1.23	94.77 ± 1.37*		0.0274	0.325	3.19
UO2-HBU-MiniF-01-23061918		10.54 ± 0.13	96.05 ± 1.21	95.73 ± 1.17*		0.0227	0.275	3.17
UO2-HBU-MiniF-01-23062819	2	10.59 ± 0.13	96.53 ± 1.22	96.52 ± 1.19*	12.42 (σ = 0.67)	0.0201	0.242	3.17
UO2-HBU-MiniF-01-23062820		10.47 ± 0.13	95.48 ± 1.21	96.72 ± 1.33*		0.0216	0.262	3.17
UO2-HBU-MiniF-01-23062821		10.61 ± 0.13	96.71 ± 1.22	95.21 ± 1.21*		0.0242	0.288	3.17
UO2-HBU-MiniF-01-23062822		10.64 ± 0.13	97.01 ± 1.23	95.64 ± 1.23*		0.0257	0.309	3.17
UO2-HBU-MiniF-01-23062823		10.56 ± 0.13	96.24 ± 1.21	96.52 ± 0.55		0.0243	0.291	3.17
UO2-HBU-MiniF-01-23062824		10.62 ± 0.13	96.80 ± 1.22	96.24 ± 0.55		0.0275	0.326	3.18
UO2-HBU-MiniF-01-23062825		10.57 ± 0.13	96.33 ± 1.22	95.38 ± 0.55		0.0253	0.306	3.17
UO2-HBU-MiniF-01-23062826		10.58 ± 0.13	96.41 ± 1.22	96.41 ± 0.55		0.0234	0.279	3.17
UO2-HBU-MiniF-01-23062827		10.60 ± 0.13	96.58 ± 1.22	96.74 ± 0.56		0.0259	0.309	3.17
UO2-HBU-MiniF-01-23062828		10.57 ± 0.13	96.32 ± 1.22	95.54 ± 0.54		0.0282	0.339	3.17
UO2-HBU-MiniF-01-23062829		10.62 ± 0.13	96.81 ± 1.22	96.45 ± 0.55		0.0255	0.305	3.18
UO2-HBU-MiniF-01-23062830		10.65 ± 0.13	97.04 ± 1.23	96.41 ± 0.55		0.0235	0.282	3.17
UO2-HBU-MiniF-01-23062831		10.58 ± 0.13	96.41 ± 1.22	96.30 ±0.56		0.0240	0.288	3.17
UO2-HBU-MiniF-01-23091936	3	10.70 ± 0.14	97.50 ± 1.24	95.56 ± 0.55	11.76 (σ = 0.18)	0.0280	0.348	3.17
UO2-HBU-MiniF-01-23091942		10.72 ± 0.14	97.76 ± 1.24	96.87 ± 0.55		0.0266	0.325	3.16
UO2-HBU-MiniF-01-23091943		10.73 ± 0.14	97.80 ± 1.24	97.01 ± 0.56		0.0296	0.356	3.16
UO2-HBU-MiniF-01-23091944		10.79 ± 0.14	98.33 ± 1.25	96.85 ± 0.55		0.0274	0.330	3.18
UO2-HBU-MiniF-01-23092045		10.72 ± 0.14	97.70 ± 1.24	97.14 ± 0.56		0.0283	0.343	3.17
UO2-HBU-MiniF-01-23092049		10.77 ± 0.14	98.22 ± 1.25	96.99 ± 0.56		0.0285	0.335	3.16
UO2-HBU-MiniF-01-23092052		10.76 ± 0.14	98.13 ± 1.25	96.51 ± 0.55		0.0295	0.353	3.16
UO2-HBU-MiniF-01-23092053		10.76 ± 0.14	98.06 ± 1.25	97.05 ± 0.55		0.0274	0.332	3.16

*Archimedes density measured on a half-pellet

4. EXPERIMENT ASSEMBLY

4.1 SUBCAPSULE ASSEMBLY

Forty-two subcapsules were successfully built. Each subcapsule was assembled and cleaned according to HFIR-approved procedures, drawings, and sketches. The material certifications and verifications for each component, along with safety-critical dimensional inspection results, were recorded in inspection request documents and approved by quality assurance (QA) representatives. The components used for each assembly are documented on fabrication requests sheets which are checked by an independent team member. Each subcapsule assembly's parts were laid out individually on a lint-free cloth, and then a checker independently verified the contents in each set to ensure that everything matched the approved fabrication request sheet. The preassembly layout of all parts of subcapsule assembly HBU02-2 is displayed in **Figure 7**. The holder and endcap are the pieces that were welded together to contain the other internal parts and the fuel specimen. Each subcapsule was assembled with its respective fuel specimen and was prepared for welding.

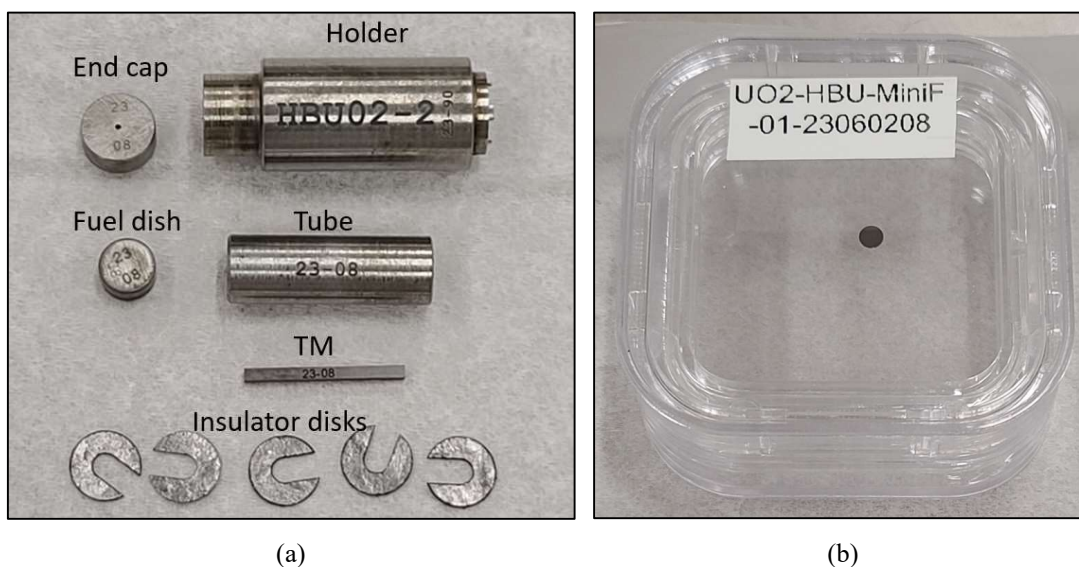


Figure 7. Example of subcapsule parts layout (a) and disk fuel specimen (b).

The first weld performed was an electron beam (EB) weld in the circumferential joint between the subcapsule endcap and holder. The subcapsules were secured into a custom-made jig and loaded into the EB welding facility vacuum chamber as shown in **Figure 8(b)**. Once the chamber was under vacuum, the endcap and holder of each subcapsule were welded together along the circumferential joint between them. Each subcapsule was then placed inside the appropriate sealed containers, which were evacuated and backfilled three times with ultra-high purity (UHP) helium gas. The small holes in the endcaps functioned as gas communication pathways between the insides of the subcapsules and the atmosphere inside the containers. The sealed containers were then placed within an air-tight glovebox that was also evacuated and backfilled to atmospheric pressure with the same UHP helium supply. The subcapsules were removed from the sealed containers inside the glovebox and secured in a vice, and the small hole in each subcapsule was seal-welded using a gas tungsten arc welding procedure.

The impermeability of the welded joints was tested through nondestructive examination (NDE) with a helium sniffer leak test and confirmation of the absence of visible bubbles when submerged in an alcohol bath under partial vacuum. Any subcapsule assembly which failed to meet the acceptance criteria for these

NDEs was cut open, placed into a new holder and endcap set, and routed back through the welding processes. These rebuilds were performed following all the necessary requirements and were documented accordingly through revisions or updates to the fabrication request sheets. Once each subcapsule's welds passed the NDE acceptance criteria, it was loaded into its respective target assembly.

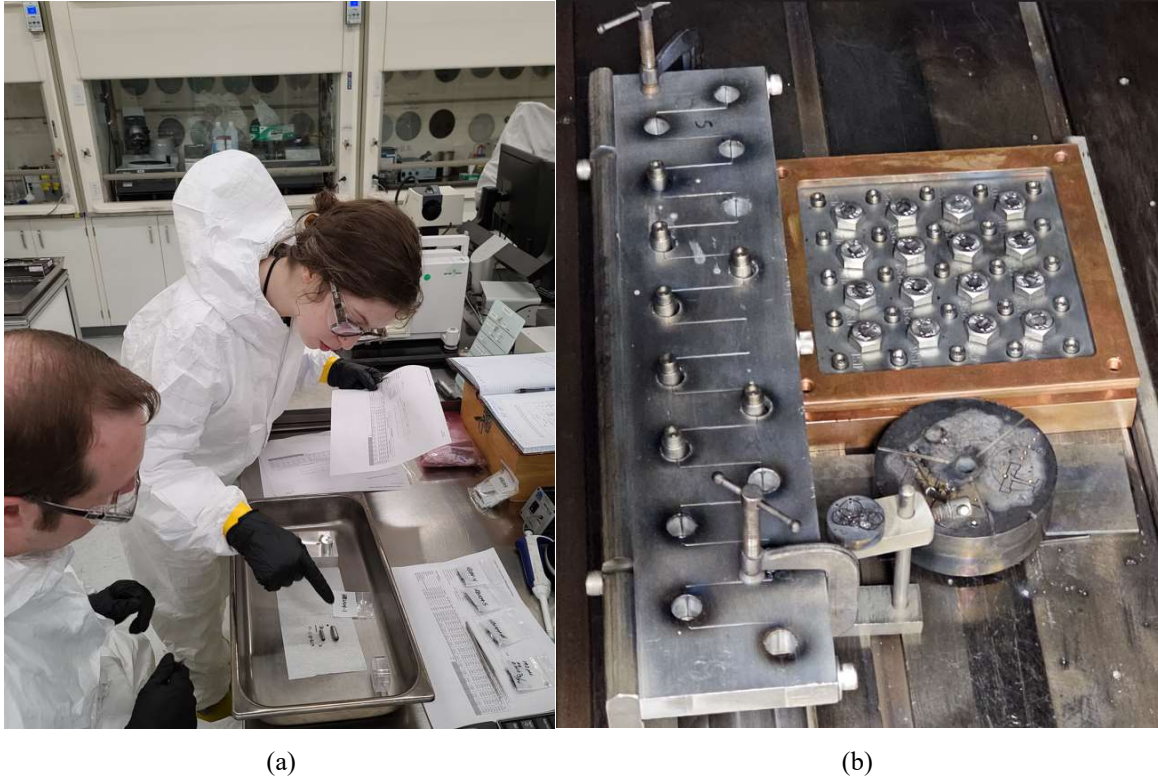


Figure 8. Subcapsule assembly step (a) and assembled subcapsules loaded into the fixture for electron beam welding (b).

4.2 TARGET ASSEMBLY

The seven MiniFuel targets were assembled, with six subcapsules loaded inside of each. The preassembly layout for a target assembly (HBU03) is shown in **Figure 9**. The parts used in each target assembly have the same documentation and cleaning requirements as the subcapsule components and were also documented and verified according to a fabrication request sheet. The target's outer tube and bottom endcap were joined together prior to target assembly using an automated orbital gas tungsten arc welding (GTAW) procedure. Once each layout was confirmed to match the fabrication request sheet by an independent reviewer, thimbles were pressed into either end of each subcapsule. The components were slid into the target's outer tube in the appropriate order, taking care to ensure the thimbles remained appropriately oriented and seated into their respective subcapsules. Once the contents were situated in the tube, the top endcap was placed against the opening of the tube, slightly compressing the top spring. Then the assembly was placed into a custom jig to hold it together until welding was performed.

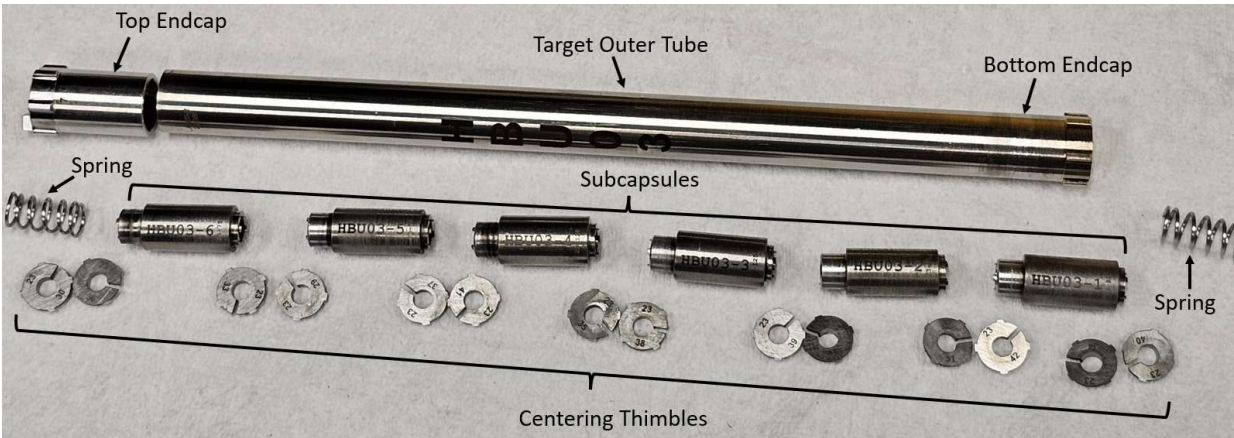


Figure 9. Preassembly target layout for HBU03.

The final welding process for target containment consisted of (1) welding the top endcap in place on the tube, and (2) sealing the gas communication hole feature in the side of the endcap. The endcap was welded in place using a manual GTAW procedure to join the endcap to the tube along the circumferential butt joint where they meet. Each target was then placed inside a sealed container, which was evacuated and backfilled with UHP helium three times. The container was placed inside a glovebox chamber which was also sealed, evacuated, and backfilled to atmospheric pressure with the same UHP helium supply. The targets were removed from their containers within the chamber and secured into a vice. The gas communication hole in the side of the endcap was sealed using a filler wire and a manual GTAW procedure. The final welded subcapsules are shown in Figure 10(a).

The containment created by the target welds was verified through the following NDE tests:

1. visual examination of the welds by a qualified weld inspector,
2. helium sniffer leak test of the welded joints,
3. holding the targets under an external hydrostatic pressure of at least 1,050 psig for 10 minutes,
4. a second helium sniffer leak test of the welded joints, and
5. dye penetrant examination of the welds.

Once each of the targets was verified to meet the acceptance criteria for these tests, the results were documented in the approval packages, and the targets were cleaned and prepared for delivery to HFIR. The list of specimens included in each target, along with their corresponding positions, is provided in **Table 4**.

Table 4. List of specimens inserted in each target and their corresponding positions.

Target ID	Subcapsule	Specimen ID
HBU01	6	UO2-HBU-MiniF-01-23060206
	5	UO2-HBU-MiniF-01-23060205
	4	UO2-HBU-MiniF-01-23060204
	3	UO2-HBU-MiniF-01-23060203
	2	UO2-HBU-MiniF-01-23060202
	1	UO2-HBU-MiniF-01-23060201
HBU02	6	UO2-HBU-MiniF-01-23061912
	5	UO2-HBU-MiniF-01-23060611
	4	UO2-HBU-MiniF-01-23060610
	3	UO2-HBU-MiniF-01-23060609
	2	UO2-HBU-MiniF-01-23060208
	1	UO2-HBU-MiniF-01-23060207
HBU03	6	UO2-HBU-MiniF-01-23062819
	5	UO2-HBU-MiniF-01-23061918
	4	UO2-HBU-MiniF-01-23061916
	3	UO2-HBU-MiniF-01-23061915
	2	UO2-HBU-MiniF-01-23061914
	1	UO2-HBU-MiniF-01-23061913
HBU04	6	UO2-HBU-MiniF-01-23062825
	5	UO2-HBU-MiniF-01-23062824
	4	UO2-HBU-MiniF-01-23062823
	3	UO2-HBU-MiniF-01-23062822
	2	UO2-HBU-MiniF-01-23062821
	1	UO2-HBU-MiniF-01-23062820
HBU05	6	UO2-HBU-MiniF-01-23062831
	5	UO2-HBU-MiniF-01-23062830
	4	UO2-HBU-MiniF-01-23062829
	3	UO2-HBU-MiniF-01-23062828
	2	UO2-HBU-MiniF-01-23062827
	1	UO2-HBU-MiniF-01-23062826
HBU06	6	UO2-HBU-MiniF-01-23091942
	5	UO2-HBU-MiniF-01-23092049
	4	35-P-21-122*
	3	UO2-HBU-MiniF-01-23092052
	2	UO2-HBU-MiniF-01-23091936
	1	35-P-21-128*
HBU07	6	UO2-HBU-MiniF-01-23091944
	5	UO2-HBU-MiniF-01-23092053
	4	35-P-21-159*
	3	UO2-HBU-MiniF-01-23091943
	2	UO2-HBU-MiniF-01-23092045
	1	35-P-21-130*

* Cr-doped depleted specimen fabricated by LANL.

4.3 MINIFUEL BASKET ASSEMBLY LOADING

The MiniFuel targets must be situated into baskets which fit into HFIR's various irradiation facilities (RB and VXF). These baskets distribute flow between the multiple channels in which stacks of targets are loaded, keeping the targets appropriately positioned with respect to the HFIR core as intended by their neutronic and thermal designs. The targets being inserted into HFIR's RB positions (HBU01 through HBU05) were loaded into a new basket assembly (MF2), which was fabricated and assembled according to HFIR-approved procedures and drawings. The MF2 basket design includes five flow channels into which the targets were loaded. These five HBU targets were positioned in the middle axial position of each basket channel, and an aluminum dummy target was placed axially above and below each target. The MF2 assembly layout with one channel loaded is shown in **Figure 10(b)**. The targets being irradiated in the VXF positions (HBU06 and HBU07) were delivered to HFIR individually and loaded into an existing basket already in HFIR.

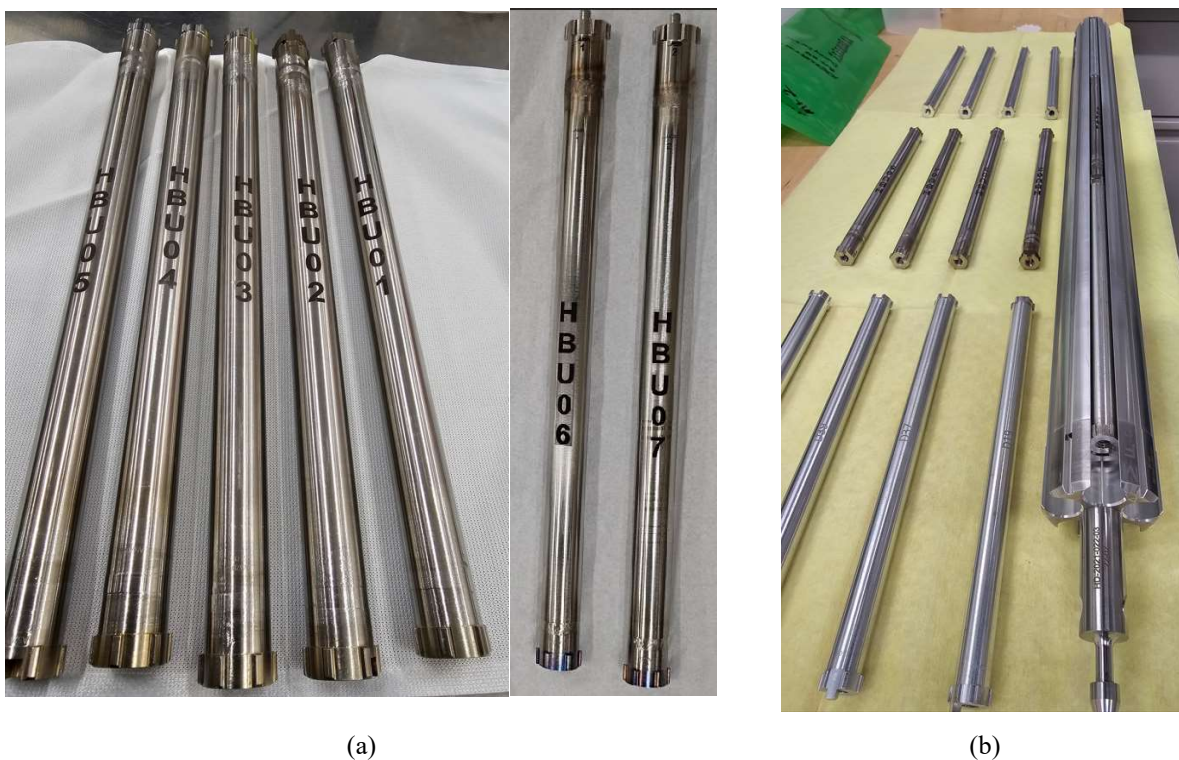


Figure 10. MiniFuel targets fully assembled (a), and RB basket assembly parts layout (b) with fueled targets, dummy targets, and RB basket.

5. HFIR INSERTION

5.1 HFIR APPROVAL PACKAGES

Every irradiation experiment that is inserted into HFIR requires an extensive fabrication package. The HBU targets were separated into two approval packages based on their respective irradiation facilities: (1) HBU01 through HBU05 and basket assembly MF2 for RB, and (2) HBU06 and HBU07 for VXF. These packages document safety-critical characteristics and were reviewed by an independent member of the Irradiation Engineering Group, a lead QA representative, and a HFIR QA representative before being

accepted for insertion into HFIR. All fabrication packages were required to satisfy all the requirements established in their respective experiment authorization basis documents (EABDs). The RB irradiation package is subject to the requirements of EABD-HFIR-2023-002, Rev. 0, and the VXF package must meet the requirements of EABD-HFIR-2018-001, Rev. 3. The documentation included in each package is detailed below:

- a bounding thermal safety analysis calculation
- the Irradiation Engineering Group review form approved by an independent engineer
- a completed assembly procedure,
- approved fabrication request sheets,
- final target dimensional inspection results,
- all inspection request documents referenced in the fabrication request sheets,
- certified weld reports for all target welds, along with relevant fill gas and filler wire certifications,
- NDE testing reports for both subcapsules and target containment,
- all relevant HFIR-approved drawings and sketches, and
- any applicable nonconformance reports or HFIR requirement deviation forms.

Because the RB and VXF targets were built in two different batches, they were completed at two different times. The RB fabrication package received final approval from HFIR on February 6, 2024, whereas the VXF fabrication package received final approval from HFIR on May 8, 2024.

5.2 HFIR IRRADIATION

The seven HBU MiniFuel targets were successfully inserted into HFIR. **Figure 11** shows the MF2 basket being loaded into an RB position in the reactor. The timeline of the irradiation is detailed for each target in **Table 5**.

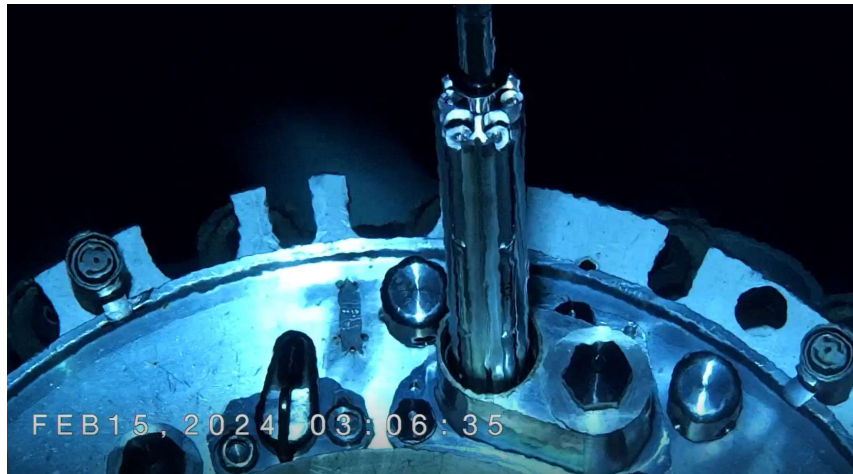


Figure 11. RB MiniFuel basket being inserted in HFIR.

Table 5. Irradiation details for the HBU MiniFuel targets

Target ID	Irradiation location	Intended number of HFIR cycles	Start of irradiation	Anticipated end of irradiation
HBU01	RB1A	7	Cycle 505 (2/27/2024)	Cycle 511 (3/14/2025)
HBU02				
HBU03				
HBU04				
HBU05				
HBU06	VXF11	16	Cycle 507 (6/11/2024)	Cycle 522 (7/2/2027)
HBU07				

6. FUTURE WORK

After the irradiation is complete, the targets will be shipped to ORNL's Irradiated Fuels Examination Laboratory for post-irradiation examination (PIE). The targets will be disassembled to recover each subcapsule. The subcapsules will be punctured to measure the fuel fission gas release. The subcapsules will then be disassembled to recover the fuel specimens and TMs. Each fuel specimen will be visually inspected. Irradiation-induced swelling will also be assessed, followed by more detailed microstructure analysis; electron backscatter diffraction (EBSD) and transmission electron microscopy (TEM) to assess the state of the grains, the porosity, and xenon bubble formation and pressure. The TMs will be shipped to ORNL's Low-Activation Materials Development and Analysis (LAMDA) laboratory to be analyzed via dilatometry and to confirm the irradiation temperatures.

7. CONCLUSIONS

To study the effect of burnup and temperature on the microstructure formations in UO_2 fuel, ORNL personnel designed a MiniFuel experiment to irradiate small UO_2 disk specimens in HFIR at various temperatures and high burnups. The goal of this experiment is to (1) investigate the dark zone burnup and temperature thresholds of UO_2 fuel specimens, (2) explore fission rate effects on the evolution of microstructure, and (3) assess fission gas release under various irradiation conditions. The MiniFuel experiment design allows for separate-effects accelerated testing of the fuel specimens. UO_2 fuel specimens were fabricated and characterized at ORNL. The densities and grain sizes of these specimens were measured and show results representative of commercial UO_2 fuel pellets. The disk specimens were successfully assembled into MiniFuel targets, and the targets were successfully inserted into HFIR in February and June 2024 in the RB and VXF positions, respectively. The first set of targets (RB targets) are scheduled to complete their seven-cycle irradiation by March 2025. After irradiation, the PIE plan includes fission gas release, swelling measurements, and fuel microstructure analysis (EBSD/TEM).

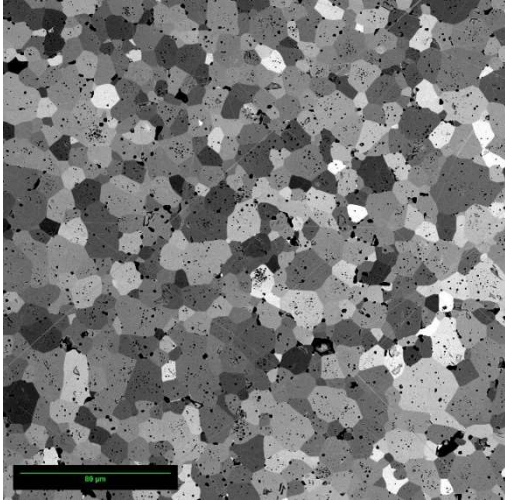
8. REFERENCES

- [1] F. Pimentel, F. Smith, “The Economic Benefits and Challenges with Utilizing Increased Enrichment and Fuel Burnup for Light-Water Reactors,” *Tech. Report, Nucl. Energy Inst.* (2019).
- [2] A Csontos, N. Capps, “Accident-Tolerant Fuel Valuation: Safety and Economic Benefits (Revision 1)”, Electr. Power Res. Institute, EPRI Rep. (2019) 3002015091. www.epri.com.
- [3] M. Bales et al., “Interpretation of Research on Fuel Fragmentation, Relocation, and Dispersal at High Burnup,” RIL 2021-13, US Nuclear Regulatory Commission, 2021.
- [4] P. Raynaud, “Fuel Fragmentation Relocation, and Dispersal During the Loss-of-Coolant Accident,” NUREG-2121, US Nuclear Regulatory Commission, 2012.
- [5] C. McKinney et al. *Advanced Multiscale Microscopy Characterization of High Burnup LWR UO₂ Before and After LOCA Testing*, Oak Ridge National Laboratory, ORNL/SPR-2023/3132, 2023.
- [6] C. M. Petrie, J. R. Burns, A. M. Raftery, A. T. Nelson, K. A. Terrani, “Separate Effects Irradiation Testing of Miniature Fuel Specimens,” *Journal of Nuclear Materials*, **526** (2019).
- [7] J. P. Gorton, Z. G. Wallen, C. M. Petrie, *Modifications to MiniFuel Vehicle to Enable Higher Temperature UO₂ Irradiation Capabilities*, ORNL/SPR-2021/2096, Oak Ridge National Laboratory, Oak Ridge, TN, August 2021.
- [8] S. C. Wilson, S. M. Mosher, C. R. Daily and D. Chandler, *HFIRCON Version 1.0.5 User Guide*, Oak Ridge National Laboratory, ORNL/TM-2020/1742, 2020.
- [9] X-5 Monte Carlo Team, *MCNP - A General Monte Carlo N-Particle Transport Code, Version 5. Volume I: Overview and Theory*, Los Alamos National Laboratory, LA-UR-03-1987, 2003.
- [10] W. A. Wieselquist, R. A. Lefebvre, and M. A. Jessee, *SCALE Code System, Version 6.2.4*, Oak Ridge National Laboratory, ORNL/TM-2005/39, 2020.
- [11] J.P. Gorton, et al., *UCN MiniFuel Irradiation Experiment: Final Design Report*, ORNL/SPR-2023/3103, Oak Ridge National Laboratory, Oak Ridge, TN, September 2023.
- [12] ANSYS, Inc., "ANSYS® Mechanical, Release 23.1," ANSYS, Inc., 2023.
- [13] A.A. Campbell, W.D. Porter, Y. Katoh, L.L. Snead, “Method for analyzing passive silicon carbide thermometry with a continuous dilatometer to determine irradiation temperature,” *Nuclear Instruments and Methods in Physics Research B*, **370** (2016).
- [14] K.G. Field, J.L. McDuffee, J.W. Geringer, C.M. Petrie, Y. Katoh, “Evaluation of the continuous dilatometer method of silicon carbide thermometry for passive irradiation temperature determination,” *Nuclear Instruments and Methods in Physics Research B*, **445** (2019).
- [15] Oak Ridge National Laboratory, *AFC Fuel Pellet Fabrication Standard Operating Guideline*, AFC-SOG-01, 2024

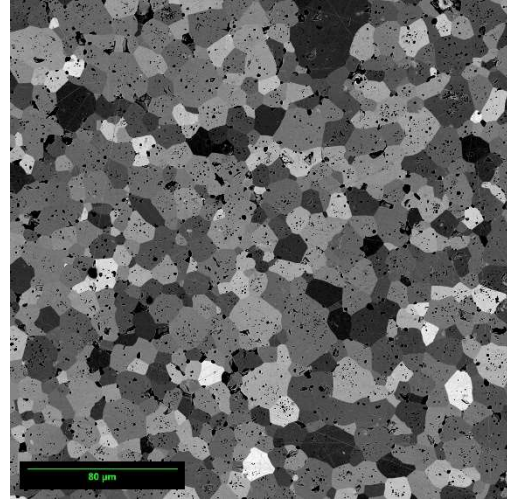
APPENDIX A. SEM IMAGES OF PELLETS

APPENDIX A. SEM IMAGES OF PELLETS

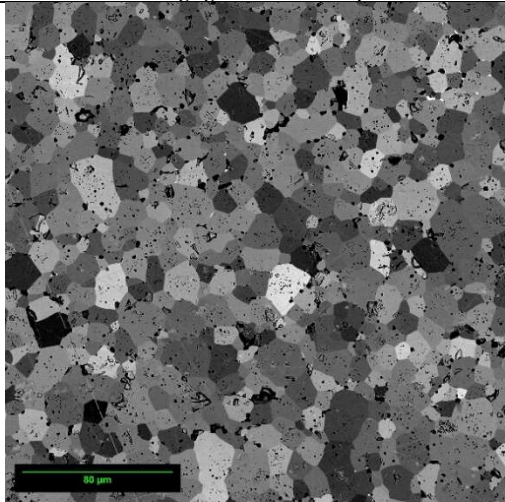
Pellets from target HBU01



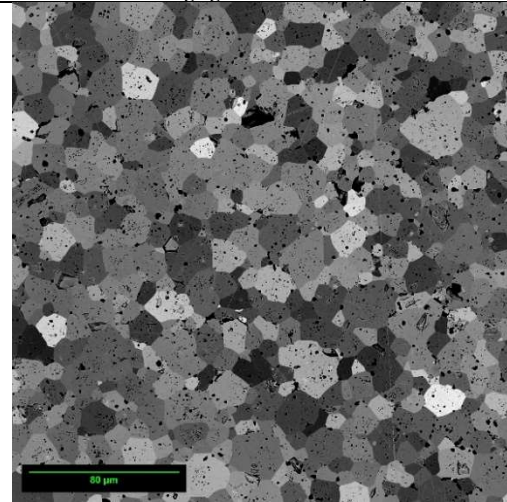
UO₂-HBU-MiniF-01-23060206
Average grain size: 12.34 μm



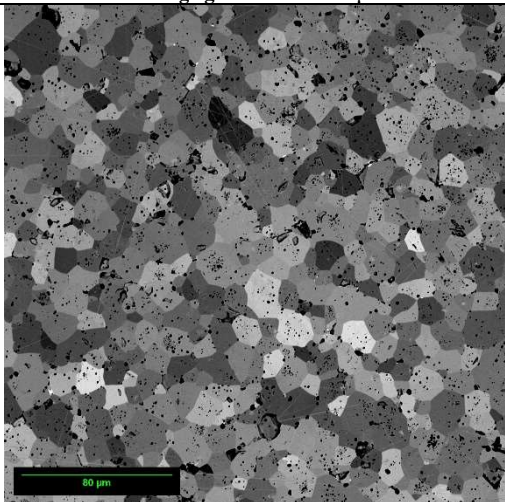
UO₂-HBU-MiniF-01-23060205
Average grain size: 11.61 μm



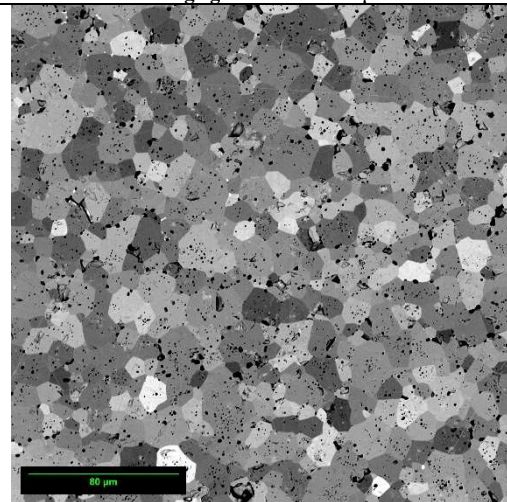
UO₂-HBU-MiniF-01-23060204
Average grain size: 11.14 μm



UO₂-HBU-MiniF-01-23060203
Average grain size: 11.49 μm

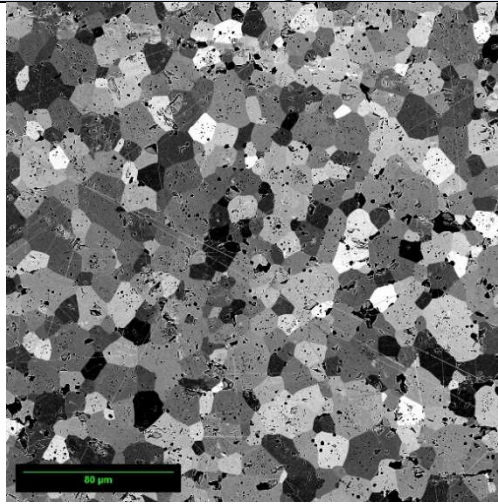


UO₂-HBU-MiniF-01-23060202
Average grain size: 11.71 μm

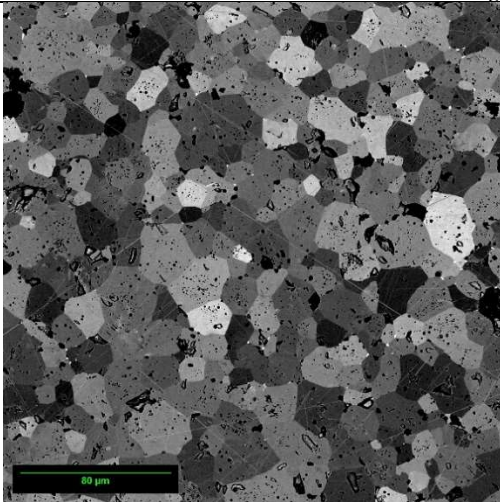


UO₂-HBU-MiniF-01-23060201

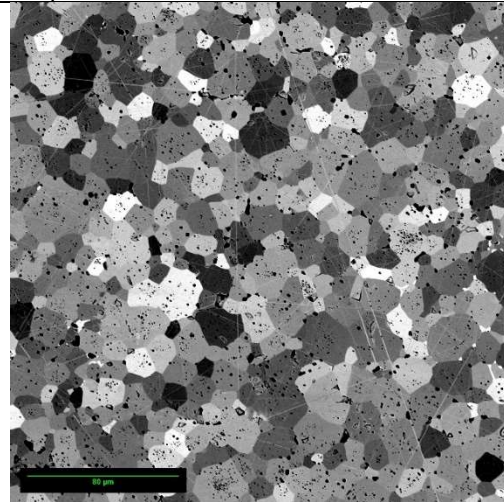
Pellets from target HBU02



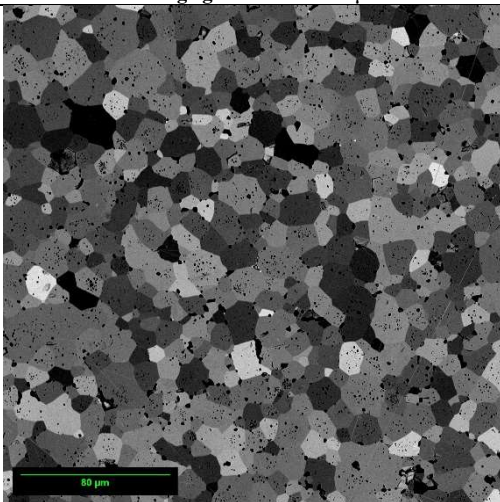
UO2-HBU-MiniF-01-23060611
Average grain size: 12.49 μm



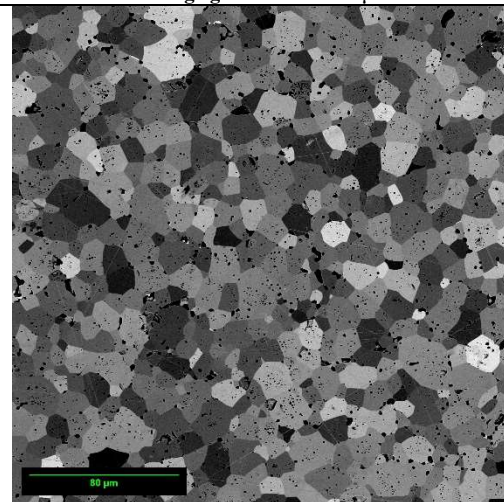
UO2-HBU-MiniF-01-23060610
Average grain size: 12.26 μm



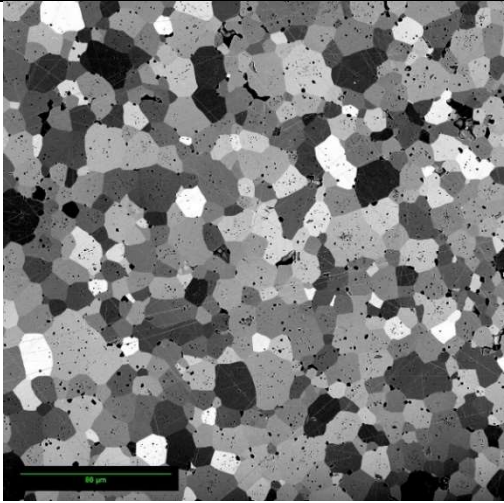
UO2-HBU-MiniF-01-23060609
Average grain size: 12.16 μm

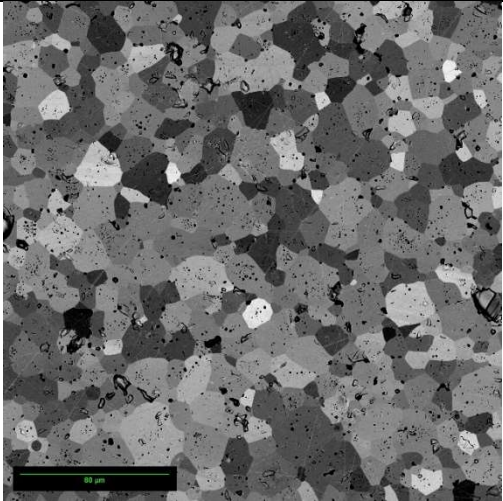
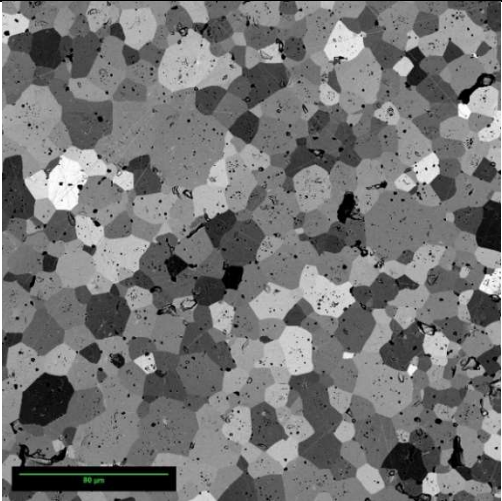


UO2-HBU-MiniF-01-23060208
Average grain size: 11.21 μm



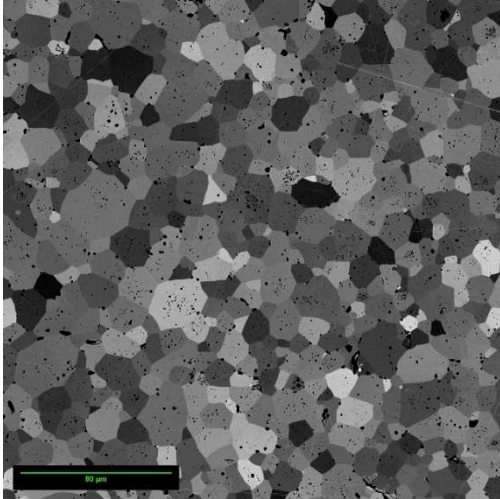
UO2-HBU-MiniF-01-23060207
Average grain size: 12.16 μm

Pellets from target HBU03	
	
	<p>UO₂-HBU-MiniF-01-23062819</p> <p>Average grain size: 11.65 μm</p>

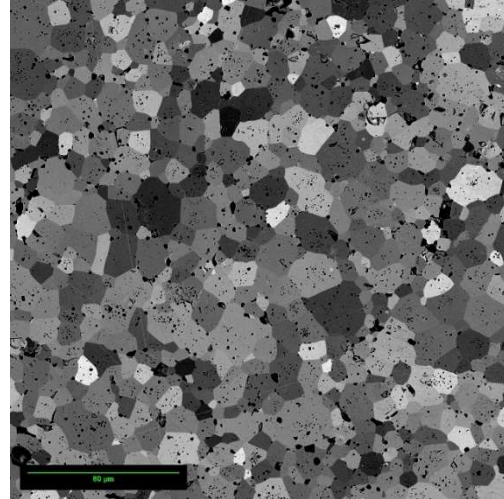
Pellets from target HBU04	
	
<p>UO₂-HBU-MiniF-01-23062821</p> <p>Average grain size: 12.72 μm</p>	<p>UO₂-HBU-MiniF-01-23062820</p> <p>Average grain size: 12.88 μm</p>

Pellets from target HBU05
N/A

Pellets from target HBU06

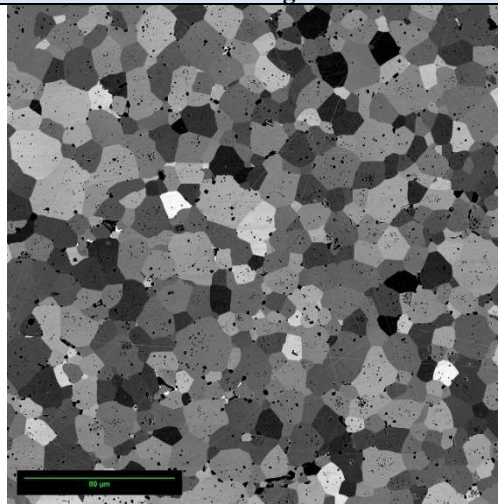


UO2-HBU-MiniF-01-23092052
Average grain size: 11.73 μm



UO2-HBU-MiniF-01-23091936
Average grain size: 11.68 μm

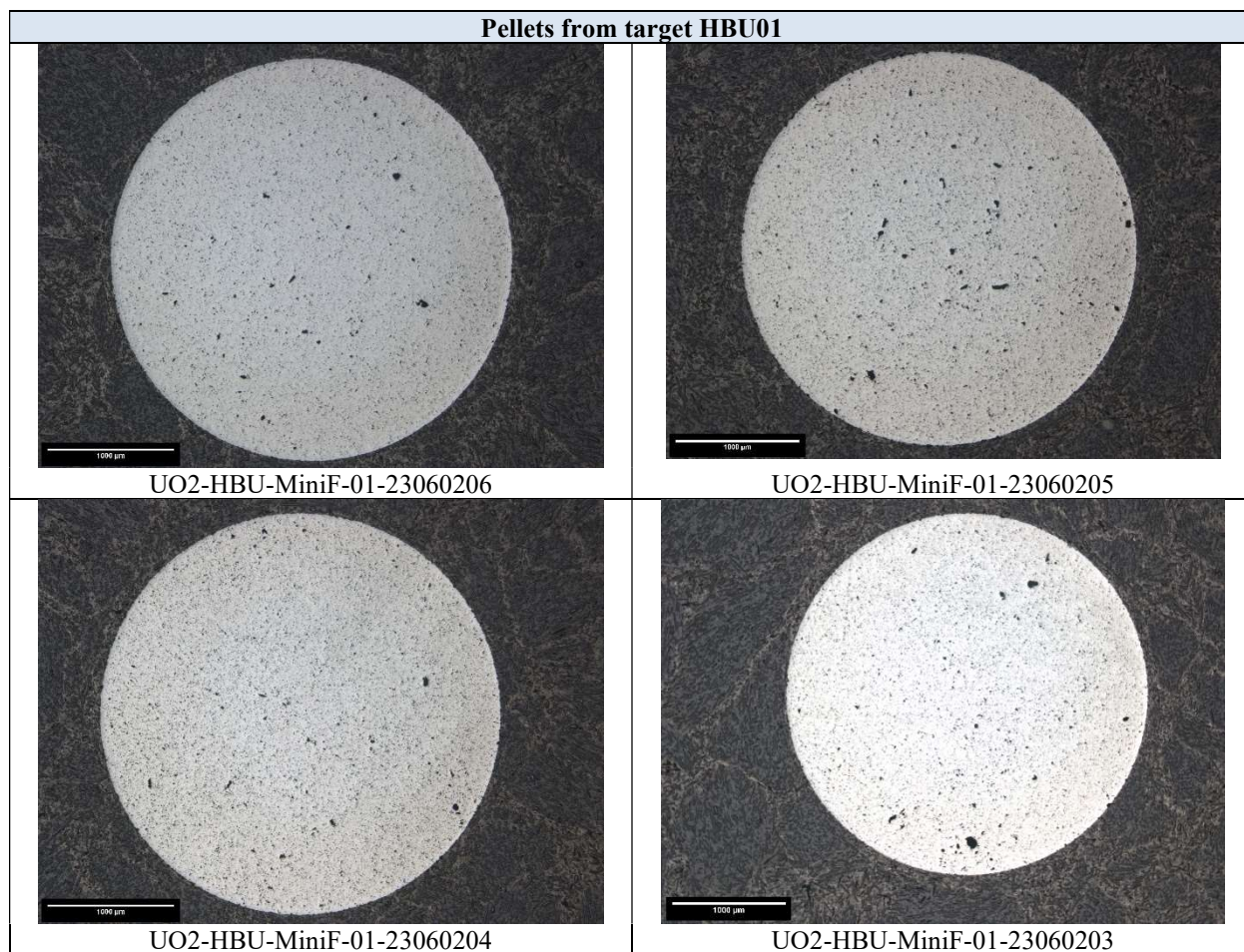
Pellets from target HBU07



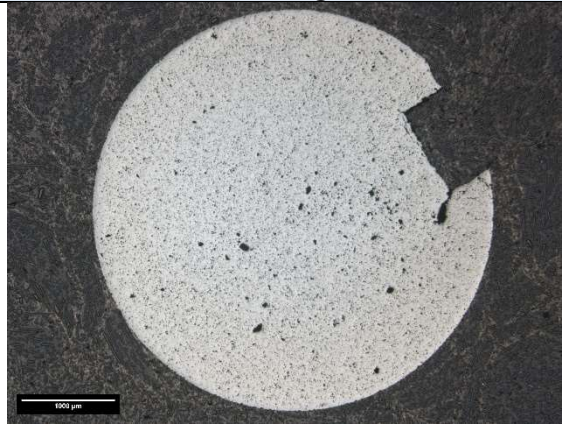
UO2-HBU-MiniF-01-23092045
Average grain size: 12.01 μm

APPENDIX B. OM IMAGES OF PELLETS

APPENDIX C. OM IMAGES OF PELLETS

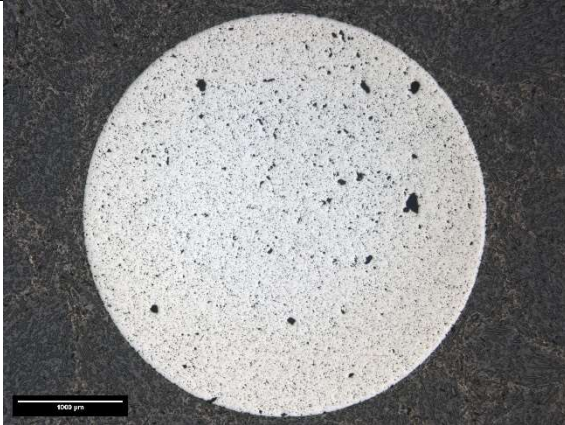


Pellets from target HBU02

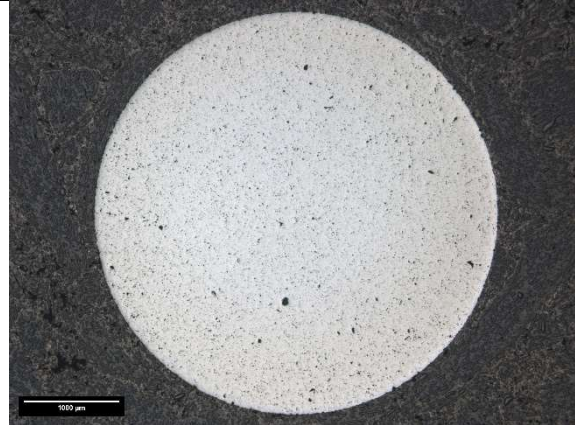


UO2-HBU-MiniF-01-23060611

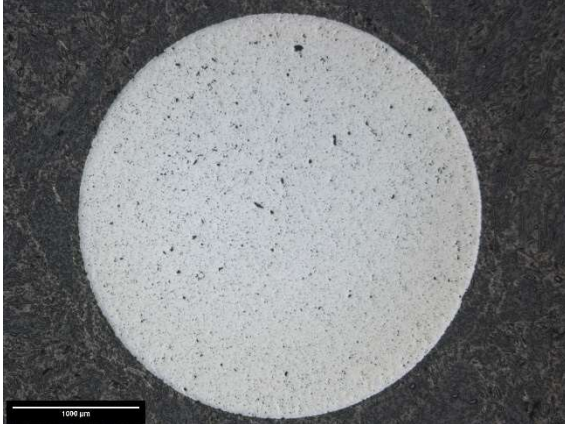
This portion of the pellets had some defects that were not present on the HFIR disks.



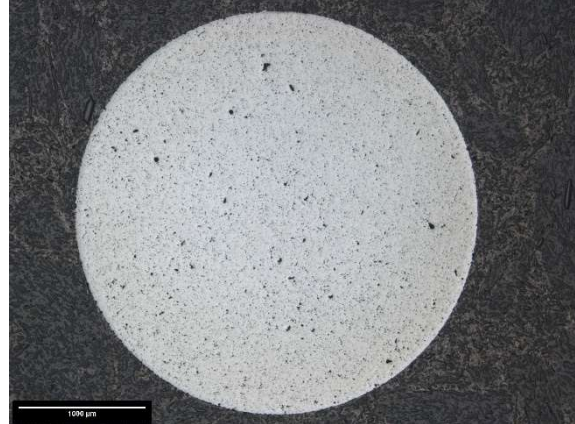
UO2-HBU-MiniF-01-23060610



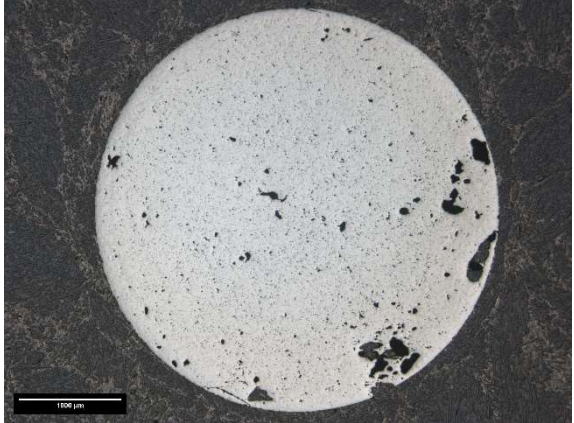
UO2-HBU-MiniF-01-23060609

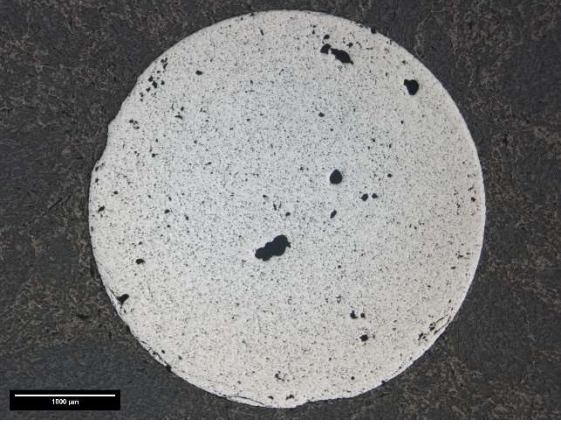
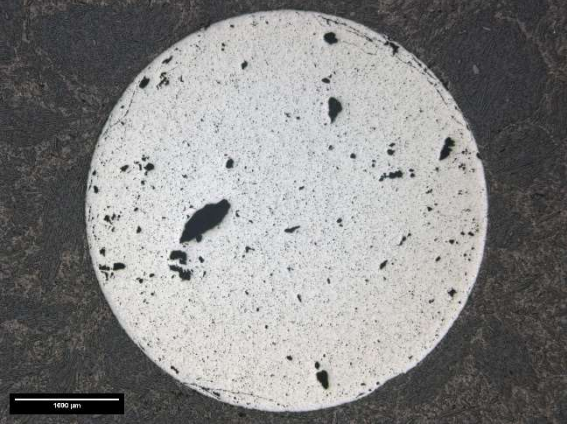


UO2-HBU-MiniF-01-23060208



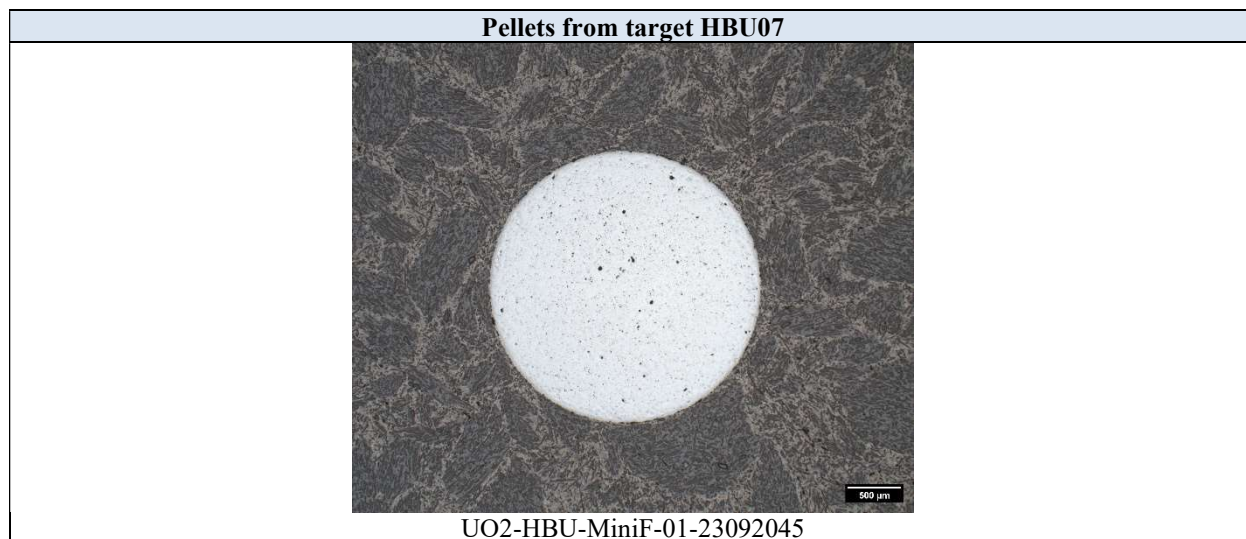
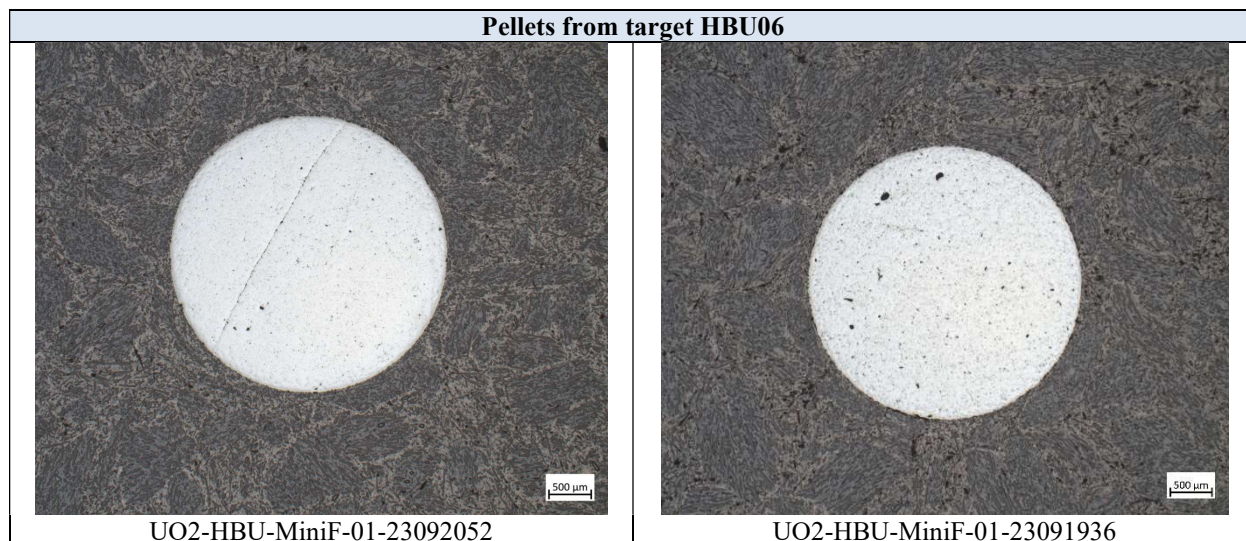
UO2-HBU-MiniF-01-23060207

Pellets from target HBU03	
	
<p>UO2-HBU-MiniF-01-23062819</p> <p>This portion of the pellets had some defects that were not present on the HFIR disks.</p>	

Pellets from target HBU04	
	
<p>UO2-HBU-MiniF-01-23062821</p> <p>This portion of the pellets had some defects that were not present on the HFIR disks.</p>	<p>UO2-HBU-MiniF-01-23062820</p> <p>This portion of the pellets had some defects that were not present on the HFIR disks.</p>

Pellets from target HBU05
N/A

Note: The following images were taken with a different optical microscope, a Zeiss Axiovert 7, and the scale bars are different than the previous images.



APPENDIX D. HFIR DISK SPECIMENS INSPECTION RESULTS

APPENDIX D. HFIR DISK SPECIMENS INSPECTION RESULTS

Specimen ID	mass (g)	Gauge Block	Thickness (mm)						Diameter (mm)			
			h1-C	h2-N	h3-S	h4-W	h5-E	h	d1	d2	d3	đ
UO2-HBU-MiniF-01-23060201	0.0255	10.001	10.307	10.304	10.311	10.316	10.306	0.308	3.19	3.18	3.18	3.18
UO2-HBU-MiniF-01-23060202	0.0231	9.999	10.271	10.266	10.284	10.275	10.283	0.277	3.18	3.19	3.18	3.18
UO2-HBU-MiniF-01-23060203	0.0228	10.001	10.281	10.266	10.280	10.281	10.266	0.274	3.17	3.19	3.18	3.18
UO2-HBU-MiniF-01-23060204	0.0260	9.999	10.314	10.314	10.304	10.306	10.306	0.310	3.17	3.17	3.18	3.17
UO2-HBU-MiniF-01-23060205	0.0280	9.999	10.331	10.331	10.342	10.332	10.342	0.337	3.18	3.18	3.18	3.18
UO2-HBU-MiniF-01-23060206	0.0300	10.001	10.365	10.365	10.361	10.361	10.360	0.361	3.17	3.17	3.18	3.17
UO2-HBU-MiniF-01-23060207	0.0275	9.999	10.327	10.323	10.340	10.320	10.345	0.332	3.18	3.19	3.19	3.19
UO2-HBU-MiniF-01-23060208	0.0217	9.999	10.265	10.266	10.255	10.253	10.265	0.262	3.18	3.18	3.18	3.18
UO2-HBU-MiniF-01-23060609	0.0188	9.999	10.224	10.219	10.237	10.227	10.226	0.228	3.18	3.18	3.18	3.18
UO2-HBU-MiniF-01-23060610	0.0249	9.999	10.304	10.306	10.288	10.287	10.294	0.297	3.18	3.18	3.18	3.18
UO2-HBU-MiniF-01-23060611	0.0246	9.999	10.294	10.292	10.298	10.293	10.294	0.295	3.18	3.18	3.18	3.18
UO2-HBU-MiniF-01-23061912	0.0236	9.999	10.281	10.283	10.273	10.284	10.274	0.280	3.21	3.20	3.20	3.20
UO2-HBU-MiniF-01-23061913	0.0244	9.999	10.298	10.299	10.292	10.295	10.287	0.295	3.17	3.18	3.17	3.17
UO2-HBU-MiniF-01-23061914	0.0262	10.002	10.313	10.312	10.316	10.314	10.313	0.312	3.18	3.18	3.18	3.18
UO2-HBU-MiniF-01-23061915	0.0254	10.001	10.312	10.308	10.309	10.312	10.308	0.309	3.17	3.18	3.17	3.17
UO2-HBU-MiniF-01-23061916	0.0274	10.002	10.327	10.327	10.327	10.331	10.322	0.325	3.19	3.19	3.19	3.19
UO2-HBU-MiniF-01-23061918	0.0227	9.999	10.278	10.290	10.266	10.273	10.265	0.275	3.17	3.18	3.17	3.17
UO2-HBU-MiniF-01-23062819	0.0201	9.999	10.243	10.243	10.243	10.226	10.252	0.242	3.17	3.17	3.17	3.17
UO2-HBU-MiniF-01-23062820	0.0216	9.999	10.262	10.261	10.260	10.260	10.260	0.262	3.17	3.17	3.17	3.17
UO2-HBU-MiniF-01-23062821	0.0242	9.999	10.284	10.290	10.284	10.292	10.284	0.288	3.17	3.17	3.17	3.17
UO2-HBU-MiniF-01-23062822	0.0257	9.999	10.308	10.308	10.308	10.307	10.307	0.309	3.18	3.17	3.17	3.17
UO2-HBU-MiniF-01-23062823	0.0243	9.999	10.292	10.288	10.290	10.287	10.292	0.291	3.17	3.17	3.17	3.17
UO2-HBU-MiniF-01-23062824	0.0275	9.999	10.325	10.318	10.331	10.327	10.323	0.326	3.18	3.18	3.19	3.18

Specimen ID	mass (g)	Gauge Block	Thickness (mm)						Diameter (mm)			
			h1-C	h2-N	h3-S	h4-W	h5-E	h	d1	d2	d3	d̄
UO2-HBU-MiniF-01-23062825	0.0253	9.999	10.307	10.314	10.299	10.300	10.304	0.306	3.18	3.17	3.17	3.17
UO2-HBU-MiniF-01-23062826	0.0234	9.999	10.280	10.266	10.288	10.273	10.285	0.279	3.17	3.17	3.18	3.17
UO2-HBU-MiniF-01-23062827	0.0259	9.999	10.307	10.311	10.306	10.312	10.306	0.309	3.17	3.17	3.18	3.17
UO2-HBU-MiniF-01-23062828	0.0282	9.999	10.341	10.341	10.336	10.332	10.342	0.339	3.17	3.17	3.17	3.17
UO2-HBU-MiniF-01-23062829	0.0255	9.999	10.304	10.304	10.304	10.306	10.304	0.305	3.18	3.18	3.18	3.18
UO2-HBU-MiniF-01-23062830	0.0235	9.999	10.284	10.276	10.285	10.278	10.284	0.282	3.17	3.17	3.17	3.17
UO2-HBU-MiniF-01-23062831	0.0240	10.001	10.288	10.293	10.285	10.289	10.289	0.288	3.18	3.17	3.17	3.17
UO2-HBU-MiniF-01-23091936	0.0280	9.999	10.347	10.346	10.347	10.347	10.347	0.348	3.17	3.17	3.17	3.17
UO2-HBU-MiniF-01-23091942	0.0266	9.999	10.325	10.325	10.323	10.322	10.326	0.325	3.16	3.16	3.16	3.16
UO2-HBU-MiniF-01-23091943	0.0296	9.999	10.354	10.360	10.349	10.351	10.361	0.356	3.17	3.16	3.16	3.16
UO2-HBU-MiniF-01-23091944	0.0274	9.999	10.332	10.327	10.327	10.335	10.325	0.330	3.18	3.18	3.17	3.18
UO2-HBU-MiniF-01-23092045	0.0283	9.999	10.342	10.345	10.340	10.342	10.341	0.343	3.17	3.17	3.17	3.17
UO2-HBU-MiniF-01-23092049	0.0285	9.999	10.336	10.333	10.331	10.340	10.328	0.335	3.17	3.16	3.16	3.16
UO2-HBU-MiniF-01-23092052	0.0295	9.999	10.353	10.353	10.350	10.351	10.351	0.353	3.16	3.16	3.16	3.16
UO2-HBU-MiniF-01-23092053	0.0274	9.998	10.330	10.335	10.326	10.331	10.330	0.332	3.16	3.16	3.16	3.16